"Implementation of the Distributed Hydrological Soil Vegetation Model (DHSVM) in West Africa: ALMIP Phase 2 project"

Kolokytha Eleni   **September-January 2013**

Stage that it has been realised at the "Laboratoire des transferts en hydrologie et environnement" (LTHE), supervised by Esteves Michel (co-supervised also by Vischel Théo and Pellarin Thierry) for the Master2 Hydrohasards.

Abstract:

In the last decades several distributed hydrological rainfall-runoff models have been developed that represent the interaction between soil and atmosphere, for the computation of the energy balance at the land surface. This component is very important in West Africa, as it plays a major role in the modulation of the monsoon system, which is the main precipitation driving mechanism at this region. In order to understand runoff generation and evolution, as well as to estimate evapotranspiration precisely enough at this region, has been implemented the physically based Distributed Hydrological Soil Vegetation Model (DHSVM). In the framework of the second phase of the AMMA Land Surface Model Intercomparison Project (ALMIP2), which aims at better analysing the reasons for the divergences of the Land Surface Models simulations, this study focuses on the ability of the selected hydrological model to simulate the hydrological processes in Benin catchment. The simulated results have been compared with validation data, which derived from the AMMA-CATCH Observatory. A focus has been given to the streamflow, due to the existence of validation data in two stations, as well has been performed a preliminary sensitivity analysis on the main hydro-dynamic model parameters.

Résumé:

Dans les dernieres décades divers modèles hydrologiques distribuées ont été développés. Ils représentent l'interaction entre le sol et l'atmosphère, pour le calcul du bilan énergétique de surface. Ceci est très important en l'Ouest- Afrique, car le bilan energetique joue un rôle important dans la modulation du système mousson, qui est le principal mécanisme à l'origine de précipitation dans cette région. Afin de comprendre la production de ruissellement et son évolution, ainsi que d'estimer l'évapotranspiration avec manière suffisamment précise, le model a base physique, le Distributed Hydrological Soil Vegetation Model (DHSVM) a été appliqué dans cette region. Cette étude s'inscrit dans la deuxième phase du programme AMMA Land Surface Model Intercomparison Project (ALMIP2), qui vise à mieux analyser les raisons des divergences entre les simulations de differents Land Surface Models. Cette étude se concentre sur la capacité du modèle hydrologique sélectionné à simuler les processus hydrologiques dans le bassin versant du Bénin. Les résultats de la simulation ont été validés avec des données provenent de l'Observatoire AMMA-CATCH. Nous nous sommes localises sur le débit, en raison de l'existence de données de validation en deux stations. A été ainsi réalisé une analyse préliminaire de sensibilité sur les principaux paramètres hydro-dynamiques du modèle.

Περίληψη :

Τις τελευταίες δεκαετίες διάφορα υδρολογικά μοντέλα έχουν αναπτυχθεί, τα οποία αναπαριστούν τις αλληλεπιδράσεις που συμβαίνουν μεταξύ του συστήματος εδάφους-ατμόσφαιρας, για τον υπολογισμό της κατανομής του ενεργειακού ισοζυγίου στην επιφάνεια του εδάφους. Αυτή η συνιστώσα είναι αρκετά σημαντική για την Δυτική Αφρική, καθώς παίζει πρωταρχικό ρόλο στη διαφόρφωση του συστήματος των μουσσώνων, οι οποίοι αποτελούν και τον κυρίαρχο μηχανισμό δημιουργίας βροχόπτωσης στην συγκεκριμένη περιοχή. Για την καλύτερη κατανόηση της απόκρισης κάποιων λεκάνων απορροής, καθώς επίσης και για τον ακριβέστερο υπολογισμό της εξατμισοδιαπνοής στην αναφερθείσα περιοχή, εφαρμόστηκε το υδρολογικό μοντέλο DHSVM (Distributed Hydrological Soil Vegetation Model). Στα πλαίσια της δεύτερης φάσης του διεθνούς προγράμματος AMMA Land Surface Model Intercomparison Project (ALMIP2), το οποίο στοχεύει στην καλύτερη διερεύνηση των αιτιών της απόκλισης των ποικίλων Land Surface μοντέλων (LSMs), η παρούσα μελέτη επικεντρώνεται στην διερεύνηση της ικανότητας του αναφερθέντος υδρολογικού μοντέλου να προσομοιώσει τις διεργασίες που επικρατούν στην λεκάνη του Benin. Τα αποτελέσματα του μοντέλου συγκρίθηκαν με δεδομένα παρατηρήσεων, τα οποία προήλθαν από το κέντρο AMMA-CATCH Observatory. Στην παρούσα εργασία επικεντρωθήκαμε στην απορροή, εξαιτίας της ύπαρξης παρατηρήσεων σε μόνο δυο σταθμούς. Επίσης έγινε και μια πρώτη προσπάθεια ανάλυσης της ευαισθησίας των κύριων υδρο-δυναμικών παραμέτρων του μοντέλου.

ACKNOWLEDGEMENTS

TABLE OF CONTENTS

1. Introduction

The continental water cycle is driven by complex interactions between atmospheric forcing (for example precipitation and temperature) and physical characteristics of the surface (such as topography and land cover). Numerical hydrological models are developed to better document these interactions. These models help to understand the role of the different processes in the modulation of the water cycle. They are also used for operational purposes as water resources or flood risk management.

In the last decades a lot of hydrological models have been developed, some are oriented for flood events modelling, other aim at modelling the interaction between soil and atmosphere, for the computation of the energy balance at the land surface (Land Surface Models-LSMs). It is however difficult to find one single model able to fully model the whole water cycle as the model are often developed for a specific objective sometime over one specific catchment.

Several inter-comparison experiments have been conducted by researchers during the last ten years in order to evaluate the performances of different hydrological models over a specified catchment or region. The principle is to provide a wide community of hydrologists with atmospheric and hydrological data over the focused region. A recent example of such experiment is the AMMA Land Surface Model Intercomparison Project (ALMIP). The international AMMA (African Monsoon Multidisciplinary Analysis) project was organized the last years with the main goal of obtaining a better understanding the intra-seasonal and interannual variability of the west-African monsoon (WAM), which is the main precipitation driving mechanism at this region. West Africa has been subjected to extreme climatic variability over the last half century, with predominantly relatively wet years during the 1950s and 1960s being followed by a much drier period during the 1970s-1990s. Populations are highly vulnerable to this climate variability. Understanding the monsoon and the surface water cycle in the region is thus an important challenge to better manage the water resources in the region.

Land surface water and energy balance has been proven to play a major role in the modulation of the monsoon system because of the strong interactions existing between the surface and the atmosphere. The modelling of the land surface component of the WAM is being addressed by the usage of land surface models (LSMs). The first phase of ALMIP consisted in implementing LSMs over the whole West African region in order to analyse the ability of the models to simulate regional water and energy balance. The results showed that the simulations differ strongly from one model to another but in absence of validation data at the regional scale, there was no possibility to rank the model performances. The second phase of ALMIP (referred hereafter to as ALMIP2) aims at better analysing the reasons for the divergences of LSM simulations. In this phase it is focused on West African sub-regions for which input data but also validation data are available for modellers. Such data are available from the AMMA-CATCH Observatory (Lebel et al., 2009), it is composed of three mesoscale sites located in a hydro-climatic gradient in Mali (Gourma), Niger (Square Degree of Niamey, 16 000 km²) and Benin (Upper Ouémé catchment, 10 000 km²) over which dense hydrological and atmospheric networks have been settled during the AMMA project.

In the framework of the ALMIP2, the goal of the present study is to determine the ability of the hydrological model DHSVM to simulate the hydrological processes in the AMMA-CATCH Benin watershed. DHSVM stands for Distributed Hydrological Soil Vegetation Model (DHSVM), it is developed at the University of Washington and Pacific Northwest National Laboratory. It is a physically based, spatially distributed hydrologic model, that was designed to provide a physically based tool for the understanding of the hydrologic consequences, especially changes in flood potential, associated with disturbances (such as logging, fire, forest roads) in forested mountainous watersheds (Wigmosta et al., 1994;Doten et al., 2006). The model explicitly solves the water and energy balance for each cell of a watershed's digital elevation model (DEM) (Figure 1, Wigmosta et al., 1994).
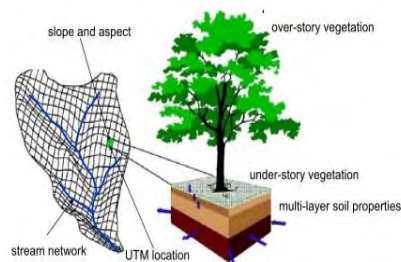
Fig. 1 DHSVM model representation of a drainage basin

DHSVM has never been applied to the Ouémé catchment, the main part of the work was thus to implement the model on this catchment by using the data provided within the ALMIP2 project.

In the first section of this report we present the region of study, we give more details about the ALMIP2 project and the data available for implementing the model. In a second section we present DHSVM. The third section will be devoted to the implementation of the model mainly by detailing the pre-processing of the data and how the model parameters have been assigned. At the fourth section we present the first simulation results and a preliminary sensitivity analysis on the main hydro-dynamic model parameters, before drawing the conclusions and the perspectives of our work in the last section.

2. Studied area and data availability

The Benin is situated in West Africa between the latitudes 6.1-12.25 and longitude 0.45-3.55. It is bordered by Togo in West, Nigeria in the east, Niger and Burkina Faso in the north. In south there is the Atlantic Ocean. It covers a land area of $112622km^2$ with a population of about 6752569 inhabitants.

2.1 Objectives

This study aims to implement and evaluate the DHSVM model in Benin watershed. Mesoscale simulations will be performed and analyzed over the Ouémé basin. The DHSVM model was applied at a 30 minutes time step for a continuous three year period, starting 1

January 2005. There are known both forcing and validation data. The first, one has to do with the micrometeorological description, as well as with soil and vegetation properties, while the second one contains surface fluxes, soil moisture, water table and runoff. Daily records of meteorological forcing such as air temperature, specific humidity, eastward and northward wind component, rainfall rate, snowfall rate, incident shortwave and longwave radiation, surface pressure and elevation relative to sea level were obtained from the ALMIP phase 2 project.

This area, as well as two other sites in Africa (Niger and Mali), are examined under the AMMA Land Surface Model Intercomparison Project (ALMIP) Phase 2 program, which is a Global Energy and Water Cycle Experiment (GEWEX). The international AMMA (African Monsoon Multidisciplinary Analysis) project was organized the last years with the main goal of obtaining a better knowledge and understanding of the intra-seasonal and interannual variability of the west-African monsoon (WAM), which is the main precipitation driving mechanism at this region. The modelling of the land surface component of the WAM is being addressed by the usage of land surface models (LSMs).

West Africa has been subjected to extreme climatic variability over the last half century, with predominantly relatively wet years during the 1950s and 1960s being followed by a much drier period during the 1970s-1990s. In addition to, this area is the world's largest source of atmospheric dust. Both the fire aerosols and dust play a major role in radiative forcing and in cloud microphysics, and thus are an important part of WAM system.

Many efforts of seasonal and interannual predictions of the west-African monsoon have been made. Although the WAM system possesses explicit zonal symmetry with characteristic jets and associated well-defined weather systems, modelling the African monsoon is not so easy, because there is appearing lack of appropriate observational datasets at sufficient space-time resolutions and because of the complex scale interactions of the respective processes at various temporal and spatial scales between the biosphere, atmosphere and hydrosphere over this region.

Generally, ALMIP deal with land surface, vegetation and hydrological models, which must be evaluated and inter-compared in order to identify key processes which are not well modelled over this region. It has been separated into two different phases, where the ALMIP Phase 2 deals with the local to mesoscales. Concerning the atmospheric point of view, the scale that is related to the hydrology of the Sahel is the convective rain scale and is the main scale of interest for agriculture. Moreover, the phase 2 has the following goals:

- Define which processes are missing or are not adequately modelled by the LSM over this region
- Investigate in which way the various LSM respond to changing the spatial scale (three scales will be analyzed: local, mesoscale and regional).
- Evaluation of the simple LSMs ability to simulate the vegetation response (mesoscale hydrology) to the atmospheric forcing on seasonal and interannual time scales.
- Investigation of the impacts of uncertainties/differences in the precipitation on the surface fluxes and hydrological responses of the LSM models.

We could say that the goal of this phase is to improve hydrology and hydrodynamics for better understanding of the water cycle. More specifically, must be able to improve Global Climate Models (GCMs) hydrological parametrizations and downscaling of GCM scenarios using hydrological models for water management issues and decision making (4th International AMMA Conference, Toulouse) (Boone A. et al., 2012).

2.2 Ouémé catchment

The Ouémé site covers a domain of 14.600 km^2 and the rainy season lasts from April to October and also the annual rainfall is between 1200-1300 mm (Guyot et al., 2009). The vegetation is dominated by wooded savannah with interspersed crops including corn and niébé. The river runoff is structured by an arborescent drainage network and conserved by the drainage of water tables. The vegetation cover is patchier than on the other sites, with forest clumps scattered in mixed fields and fallow landscape.

2.2.1 Morphology of Benin area

In general, the profile of the country is an undulating plateau with a few scattered hills in the centre and the north. The altitude varies from the sea level to 400-650 m in the northwest. Geologically the southern part refers to the West African Continental Terminal with sedimentary rock, while the northern section refers to the West Precambrian Shield with granite-gneissic rock.

2.2.2 Climate of the studied area

The mean annual rainfall varies from 900 to 1300 mm. Its lowest values are recorded in the south-western section and in the north, with values varying between 900-950mm. The highest precipitation (1200-1300) is confined to south-east. The mean annual temperatures range from 26 to 28°C and may exceptionally reach 35-40°C at the northern part. As in most West-African countries, the climate is primarily determined by the annual cycle of the Inner Tropical Convergence Zone (ITCZ). The study area, that is situated at the northern zone, is characterised by a truly Sudanian climate. The rain season lasts on average from April to October, with the optimum around August.

2.2.3 Studied domain

The spatial resolution of the grid for the forcing data is 0.05 degrees. There is used a longitude- latitude projection (is corresponding to a 28 x 25 grid). The limits for the longitude (centre of each pixel) are between 1.475- 2.825 and for the latitude are 8.975-10.175.

Fig. 2 The ALMIP (Phase 1) regional scale domain is shown. The sub-regional (mesoscale: violet outline) and rectangles containing local sites are shown: Oueme (red), Niamey (orange), and Gourma (blue). The ECOCLIMAP annual average LAI (m^2 m^{-2}) is contoured.

In addition to, the data that concern the soil and vegetation characteristics, initially were at the same resolution with the forcing data, but after were transformed at the higher spatial resolution of 0.01 degrees (the grid spacing is at 1000m and the longitude and the latitude consist of 136 and 121 components, respectively).

The grid that has been created from the provided data of the ALMIP project, were covering a grid of 16456 pixels. With the mask that was created, finally the active cells which represent our basin are 11788 pixels. Moreover, the temporal forcing uses a 30 minute time step and the data cover the period 2005-2007.

2.3 ALMIP2 data

2.3.1 ALMIP2- Meteorological data

The atmospheric forcing data for some of the parameters (air temperature, specific humidity at 2m, surface pressure and wind speed) are derived from the European Centre for Medium-Range Weather Forecasts (ECMWF) forecast data.

The original ECMWF atmospheric state variables and fluxes were at a 0.5 degree resolution on a cylindrical equidistant grid and at a 3 hour time step. The state variables were first interpolated to the 0.05 degree grid using a standard 2D approach (using an exponential distant-dependent weighting). These calculations were done by the ALMIP project team.

The surface pressure was adjusted in the same way using the hypsometric equation. Specific humidity from ECMWF at 0.5 degrees was first converted to relative humidity (RH), which was first interpolated spatially and temporally. The new specific humidity was then diagnosed on the 0.05 grid using the T_{air} and P_{Surf} on the 0.05 degree grid. State variables were interpolated in time linearly ($T_{air}, Q_{air}, P_{Surf}$). ECMWF LW_{down} was also interpolated linearly and the SW_{down} was computed using a pseudo cloud fraction using the cosine of the solar zenith angle.

The rainfall uses the best Lagrangian-krigged method, which is defined as follows: a Lagrangian methodology when coherent structures are resolved by the rain gauge network (squall lines, etc.).

Table 1 presents the atmospheric forcing parameters (the height is the distance in the atmosphere above the surface).

Variable Name	Description	Units (MKS)	Longitude	Latitude	Height	Time
Tair	Near surface air temperature	°K	x	x	x	x
Qair	Near surface specific humidity	kg/kg	x	x	x	x
Wind_E	Near surface eastward wind component	m/s	x	x	x	x
Wind_N	Near surface northward wind component	m/s	x	x	x	x

PSurf	Surface pressure	Pa	x	x	-	x
Rainf	Rainfall rate	kg/(m^2 s)	x	x	-	
Snowf	Snowfall rate	Kg/(m^2 s)	x	x	-	x
SWdown	Surface incident shortwave radiation	W/m^2	x	x	-	x
LWdown	Surface incident longwave radiation	W/m^2	x	x	-	x
Elevation	Grid box average elevation relative to sea level	m	x	x	-	-

Tab.1 The atmospheric forcing data from ALMIP project

2.3.2 ALMIP2- Soil and vegetation data

The forcing data that are related to soil and vegetation were obtained from the ECOCLIMAP II Africa database (Kaptué et al., 2010). There are various surface parameters (total number 12) (Table 2).

Variable Name	Description	Units (MKS)	Longitude	Latitude	Class	Time
patch	class fraction	-	x	x	x	-
sand	sand fraction	-	x	x	-	-
clay	clay fraction	-	x	x	-	-
rsmin	min stomatal	s.m^{-1}	x	x	-	-
droot	root depth	m	x	x	-	-
dsoil	soil depth	m	x	x	-	-
lai	leaf area index	m^2. m^{-2}	x	x	-	x
veg	vegetation fraction	–	x	x	-	x
z0v	surface roughness length	m	x	x	-	x
alb_vis	visible wavelength albedo	-	x	x	-	x
alb_nir	near infrared albedo	-	x	x	-	x
emis	emissivity	-	x	x	-	x

Tab.2 The soil/vegetation forcing data from ALMIP project

3. DHSVM-Model description

3.1 Hydrological cycle and modelling

The last decades, modelling has become a widely used research tool, as it helps to understand the components of the hydrologic cycle and to predict the hydrologic responses to potential anthropogenic impacts. The objective of hydrologic models is to represent the physical processes within each watershed of interest. Driven by atmospheric forcing and for known catchment's physical characteristics the models generate streamflow hydrographs at the basin outlet that reproduce the corresponding observed hydrographs. In the last decades several distributed hydrological rainfall- runoff models have been developed, that depict the interaction between soil and atmosphere, for the computation of the energy balance at the land surface (Land Surface Models-LSMs) (TOPMODEL (Beven and Kirky, 1979) and TOPKAPI (Ciarapica, 1998)). But although the physical processes governing the hydrologic cycle are generally well understood, the ability of scientists to model these

processes is more limited and many times the models are unable to follow the runoff evolution in time and estimate evapotranspiration precisely enough.

The driving force of the hydrological cycle is the incoming energy from the sun, which is generally considered to begin with the evaporation of water from oceans. The resulting water vapor is transported to the atmosphere and can produce precipitation under some conditions. Precipitation may be intercepted either by the vegetative canopy or can fall through the canopy directly to the soil. Vegetation influences the hydrological cycle through the exchange of energy, water, carbon and many other substances and is therefore critical for many hydrological processes, in particular transpiration, infiltration and runoff.

Water on the tree can be evaporated directly back to the atmosphere, fall to the ground as throughfall or flow along stems to the ground as stemflow (flow of intercepted water down the trunk or stem of a plant). When precipitation reaches the soil it will infiltrate into the soil, evaporate from the soil surface or become surface runoff (overland flow).

The movement of water through the hydrological cycle varies significantly in both time and space. The emphasis in hydrology is given in four phases: precipitation, evapotranspiration, surface runoff and ground water.
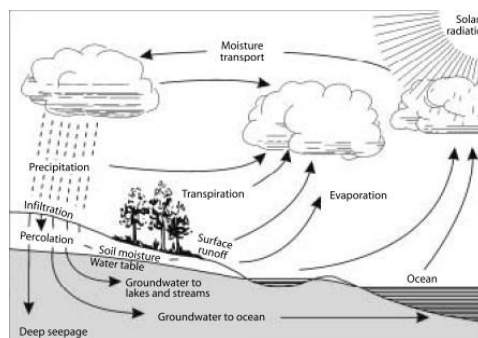

Fig. 3 The hydrological cycle

The runoff will occur either the soil is saturated and there is no more space for water storage in the soil profile or the rate of precipitation exceeds the infiltration capacity and thus water is falling at a faster rate than the soil infiltration capacity.

3.2 Principle of the DHSVM model

If the runoff occurs, it could be surface runoff (overland flow), subsurface flow (interflow) and groundwater runoff (base flow). Overland flow is the water that travels over the surface of the ground towards the stream channel. It can be generated by two mechanisms, either the infiltration excess runoff (Hortonian overland flow) (Fig. 4-pixel 3) or saturation excess runoff (Fig.4 pixels 6 and 7). The DHSVM model calculates infiltration into the upper soil layer based on the maximum infiltration rate, which is defined by the user. Infiltration excess runoff often occurs from patches where soils become saturated at the surface. This happens when rainfall intensity exceeds the infiltration capacity of the soils. Saturation excess runoff is generated by rainfall on areas where the soil is already saturated from below.

This flow occurs when the amount of throughfall and snowmelt exceeds the user defined infiltration capacity of the soil. It could also be generated if throughfall or snowfall occurs for a grid cell that already represents a fully saturated soil layer. Also, return flow from a water table rising above the soil surface, is capable to generate surface water for routing in DHSVM (Wigmosta et al., 1994, Wigmosta et al., 2002).
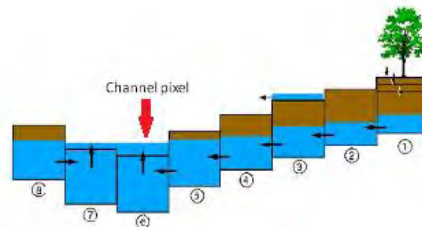

Fig. 4 Runoff generation and routing

Subsurface runoff represents the portion of infiltrated rainfall that moves laterally through the upper soil layers until it reaches the stream channel. Subsurface runoff moves more slowly than surface runoff. The proportion of total runoff that occurs as subsurface runoff or interflow depends on space and time properties of rainfall and physical characteristics of the catchment. Saturated subsurface water movement is controlled in DHSVM by the transmissivity of an individual grid cell, as determined by the lateral saturated hydraulic conductivity of the soil profile.

The last category, which is the baseflow, is the portion of infiltrated rainfall that reaches water tables and then discharges into streams, represents the drainage of water to the streamline from the regional or deep groundwater, or both.

3.3 Physically based distributed modelling

Every hydrology model is designed for specific simulation goals. In our case, models like the DHSVM or TOPMPDEL (Beven et al., 1993) are used for modelling flow in forested watersheds. Hydrologic watershed models (deterministic) could be characterized either lumped or distributed. A lumped model considers the physical characteristics of the watershed to be uniform. Distributed models are more complex as they account for the watershed as it physically occurs in the landscape. More specific, physically based distributed modelling is based on the hypothesis that the spatially distributed data are related to the model parameters, so there is theoretically little need for model calibration. These types of models were developed in an attempt to explicitly address the complicated interactions between the atmosphere, topography, soil, water and vegetation in every watershed. These models represent the spatial variability of the atmosphere and land surface characteristics that control the rainfall-runoff process, divide a watershed into grid cells and connect all cells to form a drainage network. Distributed models have an advantage in comparison to the other category of deterministic models, over their ability to disaggregate the source of streamflow to ungauged locations upstream of the calibration location. It justifies the utility of the DHSVM model to ungauged catchments and its use in climate change (Vano et al., 2009).
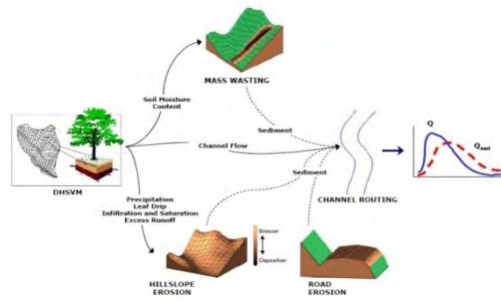
Fig. 5 Sediment module schematic

These models find many applications, for instance are used for prediction of the erosion and sediment transport in forested watershed, like the sediment model that represents analytically the sources of sediment generation within the DHSVM environment (mass wasting, hillslope erosion and road surface erosion (Figure 5, Doten et al., 2004). One parameter that is interdependent and affects the surface erosion and mass wasting is the vegetation removal.

3.4 Model structure and processes approach

The DHSVM model is a spatially explicit hydrological model that takes into account the movement of water on and through the landscape for the physical processes with a distributed, deterministic approach. It was designed for mountainous watersheds (Wigmosta et al., 1994) and dynamically makes a representation of the spatial distribution of evapotranspiration, snow cover, soil moisture and runoff through a watershed. It is able to simulate runoff, route the movement of sediment and water through the landscape and capture locations that are apt to mass wasting failure.

The model explicitly solves the water and energy balance for each cell of a watershed's digital elevation model (DEM). The modeled landscape is divided into computational grid cells that are centered on DEM elevation nodes. Digital data are used to model topographic controls on incoming solar radiation, air temperature, precipitation and downslope movement. Linked one-dimensional moisture and energy balance equations are solved irrespective for every model grid cell.

Grid cells are potentially able to exchange saturated subsurface flow with their eight adjacent neighbours, allowing for a three-dimensional representation of surface and subsurface water interactions across the landscape. Return flow and saturation overland flow are happening when the cell's water table intersects the ground surface. Unsaturated movement through the rooting zone soil layers is calculated by using Darcy's law. The spatial distribution of canopy interception, evapotranspiration, soil moisture, water table depth, snow distribution and melt, as well as runoff production can be simulated at hourly or longer time steps.

The model uses a two layer canopy representation for interception and evapotranspiration, a two-layer energy balance model for snow accumulation and melt, a multi-layer unsaturated soil model and a saturated subsurface flow model. Digital elevation data are used to model topographic controls on solar radiation, precipitation, air temperature and

downslope water movement. The DHSVM model, predicts soil infiltration, storage, surface runoff and saturated subsurface flow for each pixel over a user defined time step. Total stream flow can also be predicted at the basin outlet.

The model has improved significantly the last years and differs from the original version that was described in Wigmosta et al (1994). Canopy snow interception and release can be simulated and the two-layer ground snowpack representation replaced the one-layer, increasing the accuracy. A three dimensional overland flow representation has been added, as well as the ability to simulate the impacts of roads on downslope water redistribution (Wigmosta et al., 2002).

The DEM is the basis for the model structure, because it provides the topographic controls required by the model for the calculations. Moreover, characterization of soil and vegetation at the DEM resolution, results the topographic controls on absorbed solar radiation, precipitation, air temperature and downslope water movement in the model.

The model is using both a two-layer vegetation representation and a multi-layer soil profile representation. As it was written previous, for each pixel that is in the selected watershed boundary, it is given a single soil and vegetation class. In each model pixel, the land surface consisted of overstory vegetation, understory vegetation and soil. The overstory may cover all or a specified fraction of the land surface. The understory, if present covers the entire ground surface. The model allows land surface representations that range from a two-story forest to bare soil. Meteorological variables (like precipitation, air temperature longwave and shortwave radiation) are prescribed at a specified reference height above the overstory.

Moreover, accurate representation of the vegetation is important, because vegetation presence and structure, affects many parameters, such as temperature, moisture, wind and radiation. Because of the existence of the two canopies, there is appearing attenuation at the values of solar radiation and wind speed. In cases that there is presence of snow, it is hypothesized to cover the understory. It will have as consequence to affect the radiation transfer and the profiles of the wind across increased values of albedo and decreased surface roughness. Solar radiation and wind speed are attenuated through the two canopies. In case that there is snow, it is assumed to cover the understory and by this way it influences radiation transfer and the profile of the wind (increased values of albedo and decreased surface roughness).

An independent one-dimensional water balance is calculated for every pixel (Fig. 6(a)). Water balance is based on the law of conservation of mass, which says that any change in the water content of a given soil volume during a specified period, must be equal to the difference between the amount of water added to the soil volume and the amount of water withdrawn from it. So, the water content of the soil volume will increase when additional water from outside is added by infiltration or capillary rise and decrease when water is withdrawn by evapotranspiration or deep drainage.

Finally, the soil/vegetation water balance (Wigmosta et al.,1994) for each grid cell is:

$$\Delta S_{s1} + \Delta S_{s2} + \Delta S_{io} + \Delta S_{iu} + \Delta W = P - E_{io} - E_{iu} - E_s - E_{to} - E_{tu} - P_2 \, ,$$

where at the left side of the equation are described the changes in storage, while at the right side there are appearing the input and the outputs. More specifically, ΔS_{sj} (where j=1,2 for the upper and lower rooting zone, respectively) are the changes at the rooting zone soil water storage, ΔS_{io} and ΔS_{iu} are the changes in overstory and understory interception storages, respectively, ΔW is the change in snowpack water content, P is the volume of precipitation, P_2 is the discharge volume leaving the lower rooting zone, E_s is the volume of surface soil evaporation and E_{io}, E_{iu}, E_{to}, and E_{tu} are the volumes of overstory and understory evaporation from interception and transpiration. The water that is leaving the lower rooting zone (P_2), recharges the local water table.

DHSVM first calculates evaporation of intercepted water from the surfaces of wet vegetation, which is assumed to occur at the potential evaporation rate. Transpiration from dry vegetative surfaces is calculated using a Penman-Monteith approach. In the absence of the understory, evaporation from the upper soil layer is then calculated, as function of the potential evaporation rate, the soil moisture content, soil type and previous moisture conditions.

Then, the model makes calculations which address to the downward vertical moisture transfer moving from top to bottom through the soil profile. Evapotranspiration is modeled through a stepwise approach, by a way that allows the vegetation surface to go from wet to dry during a time step (Wigmosta et al., 1994). From these calculations, the model checks whether the amount of total evaporation from both vegetation layers, does not go beyond the amount of moisture that the atmosphere absorbs (for example, rate of potential evaporation from the overstory layer) (Wigmosta et al., 2002). The overstory can remove water from the upper as well as the lower soil zone, in comparison to the understory which is permitted to remove water only from the upper zone.

As water is moving downslope toward a stream channel it may be intercepted by a road network (Fig. 6(b)). This water continues moving through the road drainage network, up to the time that it reaches a culvert or stream channel. Discharge from culverts without a defined channel is subject to re-infiltration as it moves downslope below the culvert.
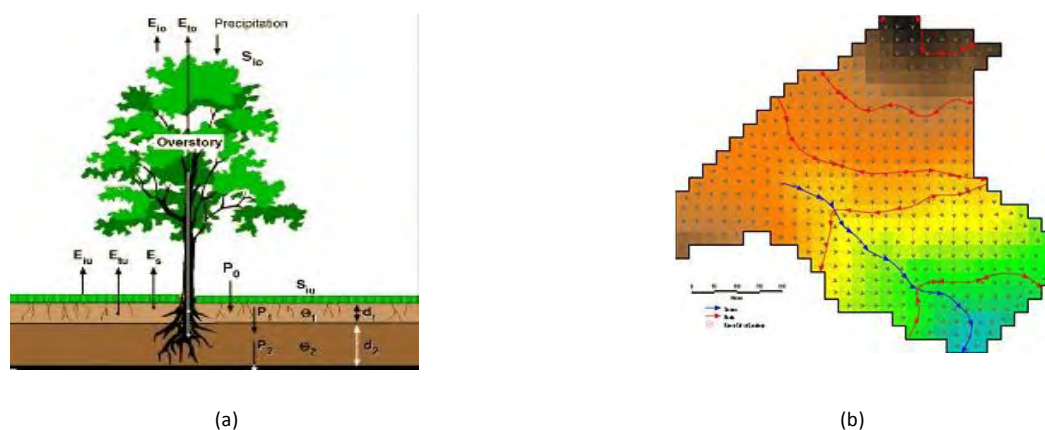

(a)   (b)

Fig. 6 Water balance (a) and model representation of hydrologic features (flow directions, road locations (red line), drainage directions, culvert locations and stream channels (blue line)) (b)

Vertical unsaturated moisture movement through every soil layer is calculated under the hypothesis of a unit hydraulic gradient and a constant vertical saturated hydraulic conductivity in each layer. Of course, it is possible to vary the saturated hydraulic conductivity at the different layers. Percolation from the lowest rooting zone recharges the grid cell water table. Every DEM grid exchanges saturated subsurface flow with its eight adjacent neighbours, according to the local hydraulic gradient. By this way, there is a three-dimensional representation of saturated subsurface flow. Return flow and saturation overland flow are produced in locations where the grid cell water tables intersect the ground surface.

Then, water is transported to the basin outlet using an explicit surface runoff and channel routing scheme, that takes information about the location, from stream channels and road networks (Bowling and Lettenmaier., 2000). These networks directly intercept precipitation and subsurface flow.

The presence of vegetation is crucial because it affects the streamflow (through evapotranspiration processes and by the interception of precipitation). If it is removed, there will be ignored a very important parameter, the leaf area index (LAI) and then there will be noted a decrease in evapotranspiration. If something like this happens, then there will be an increase in soil moisture having as consequence the increase in peak flow and baseflow at the catchment.

3.5 Model discretization

Topographic data, meteorological time series and land surface data, are required as input data from the model. Topographic data have to do with the watershed delineation and flowpath, and include stream channel information (class, map and network). Concerning the meteorological data, the model needs data for nine parameters: air temperature, relative humidity, incident shortwave and longwave radiation, wind speed, rainfall, surface pressure, lapse rate temperature and terrain (elevation data).

DHSVM requires specification of soil and vegetation information. For every pixel within the watershed boundary, a single soil class and vegetation type is assigned. To parameterize the model using physical data, there was needed the creation of vegetation classification, where the land surface is comprised of the overstory, that may cover all or a defined fraction of the land surface, and understory vegetation, which covers the entire land surface. Moreover, something similar was needed from the model for the soil (identification of the predominant soil types). The soil texture was based on the USDA classification, which was developed by the United States Department of Agriculture and the data are based on Food and Agriculture Organisation of the United Nations (FAO) and are in 10 km spatial resolution.

Solar radiation and wind speed are attenuated through the two canopies. In case that snow is present, it is assumed to cover the understory and by this way affects radiation transfer and the wind profiles via high values of albedo and a reduction of the surface roughness.

The DHSVM simulation provides a number of different types of output. The file that is always resulted, is the mass balance file which contains the various water balance components and water balance error for each individual time step (such as runoff, saturated subsurface flow, channel interception, precipitation, evapotranspiration, soil moisture and sublimation).

3.6 DHSVM applications

The DHSVM model has been implemented successfully in many watersheds the last two decades (Doten et al., 2004; Storck et al., 1998; Whitaker et al., 2003). It has been developed and verified by Wigmosta et al. (1994) in north-western Montana and more specifically at the Middle Fork Flathead River basin. The model has been implemented at a 180 meters grid, with a three hours time step and the discharge that has been generated from the model, was in agreement with the observed.

Storck et al., (1998) wanted to assess the hydrological effects of logging in the Pacific Northwest. For this reason, they applied the model to three different watersheds in Washington (North Fork Snoqualmie, Little Naches and Hard and Ware Creeks). The model simulation results showed that the first catchment, which is dominated by rain-on-snow events during the winter, is more sensitive to forest harvest practices at low in comparison to mid-elevations. In the Little Naches basin, the spring snowmelt area at higher elevations is most sensitive to forest harvest. An increase in response time to storms with greater forest road networks occurred in Hard and Ware Creeks catchment. The calibration years for the catchments contained large floods that exceeded the one hundred year flood return periods, but the study suggested that the flooding was maybe due to forest harvesting practicing and not only to climate variability.

Morover, the model has been applied at the LTHE laboratory for hydrological and suspended sediment modeling in the lake Tana Basin in Ethiopia (Michel Esteves and Agizew Nigussie Engida, 2010). In addition to, except of the use of the DHSVM model in hydrologic analysis, modelling and applied research at forest management activities, it was also used to study the interactions between climate and hydrology (Wigmosta et al., 2005) as well as the potential impacts of climate change on water resources (Wigmosta et Leung, 2000).

4. Model Implementation

4.1 Technical modifications

The distributed hydrology soil vegetation model is a highly parameterized model, which requires extensive inputs. For the formation of the suitable maps (inputs), the files were redacted and elaborated with the aid of the statistical language/environment 'R package', which is used for statistical computing and graphics. R package is a very useful tool which provides a wide variety of statistical and graphical techniques, such as linear and nonlinear modelling, classical statistical tests, time series analysis and clustering.

The selected type that was created, for being the model able to read our maps, was the NetCDF (Network Common Data Form) format. It is a set of interfaces for array-oriented

data access and its libraries support a machine-independent format for representing scientific data. It has the advantage that includes information about the data it contains (information about the dimensions, the names, units and type of the variables).

4.1.1 Model Inputs and outputs

For the simulation, DHSVM requires information about meteorology and land surface. A schematic representation of all the needed parameters, it is shown (Fig.7). Parameters are time invariant and describe the unchanging properties of the basin or model elements. They are also related to physical properties of the basin, including soil, topography, land cover and channel geometry. The mapping from soil texture classes and land cover types to model them is through a set of value attribute lookup tables, which associate a model parameter value with each grid cell.

The DHSVM model inputs could be divided in three different categories. First of all, it is needed from the model time series data. These data consist of the meteorological data at a specified time step (in our case, the data that were taken from ALMIP project have three hours time step). The next category is comprised by the spatial characteristic data, which are parameters that vary cell by grid cell but do not change over the period. They include parameters related to topography (the digital elevation model (DEM) and the watershed mask) and also soil and vegetation parameters (formation of three different maps: grids of vegetation, soil and soil depth type). The last one that is needed, are data that include information about stream and road networks.
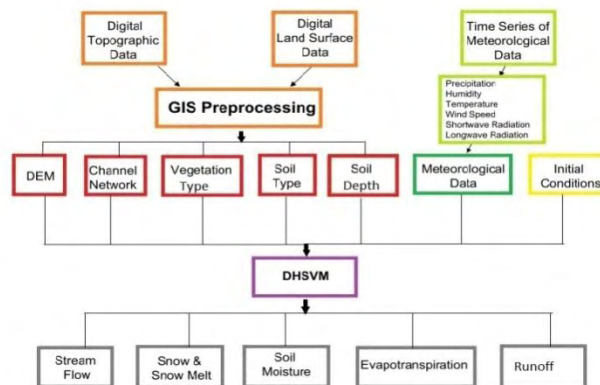

Fig. 7 DHSVM input and outputs (Storck, 2000)

For this purpose there were formed five NetCDF files (for vegetation, soil, soil depth, DEM and Mask). Moreover, there were created also and other nine files for some meteorological data (relative humidity, precipitation, temperature, wind, pressure, lapse rate temperature, terrain, shortwave radiation and longwave radiation).

The values of the atmospheric variables, derived from the atmospheric forcing data, where for the first four variables were applied transformations which will be referred precisely thereafter and concerning the lapse rate temperature, there was assumed a uniform value of 0.0065°C/m.

Unfortunately, initially the model wasn't capable to read the data from the NetCDF files. The problem derived the incompatibility at three points. The first one had to do with the format type of the variable. The valid options from the R package were the following five: short, integer, single, double and char. But from the model, the compatible types are byte and float for the different parameters (Table 3).

Input file	Name of variable	format
Soil	Soil.Type	byte
Vegetation	Veg.Type	byte
Mask	Basin.Mask	byte
Soil depth	Soil.Depth	float
DEM	Basin.DEM	float

Tab. 3 Input characteristics concerning the format

The second one, had to do with the parameters that were defined in two dimensions, and from the model there was needed also the time dimension. Regarding the last one, is related with the order of the variables and dimensions.

The solution that was selected for overtaking this problem was to change manually the previous points. It was held with the aid of the LINUX environment (the specific commands that were used were ncdump, gedit and ncgen).

The previous maps and files have been created for being used at the configuration file, which is an ASCII text file that acts as a look-up table for the physical values describing the spatial inputs into the model. At this file, we define the paths for the inputs as well as all the necessary parameters for the model running (model area, time, constants, terrain information, stream network, road network, meteorology, soils information, vegetation information and model maps that we want to be created).

The model doesn't have a limitation about the number of soil and vegetation types in a watershed. Moreover, each soil type may consist of any number of soil layers (the most used are three) and vegetation type can be segregated in different root zone layers. In our case study, although we define that we have 3 different soil layers, we put the same values because we hypothesized that we have homogeneous soil. Regarding the vegetation, we assumed that we have only one root zone layer.

Soil hydraulic properties are necessary for various studies of water and solute transport, but there are many times that is very difficult to be measured because of many constraints. The list of the DHSVM model inputs that includes the physical values, describing each individual soil and vegetation type, is long. There was a difficulty to find the values of all these parameters, especially in the case of vegetation. Some of them are incomprehensible and there wasn't the knowledge of some other for computing them. In addition to, there was a gap in available literature for each unique soil and vegetation type, for taking some values directly from the bibliography.

4.1.2 Leaf Area Index (LAI) and albedo indices

➢ Leaf Area Index (LAI)

Two other important parameters that it was necessary to computed, depending on vegetation (concerning the fraction of vegetation) are the Leaf Area Index (LAI) and the minimum stomatal resistance. The LAI is the total one-sided area of all the leaves above a given ground area divided by the ground area. It is given in $m^2 \, m^{-2}$.

The amount of leaves in the canopy is a factor in determining the amount of light intercepted by the canopy, which in turn controls photosynthetic rates. Leaves contain pores, called stomata, through which carbon dioxide and water pass between the plant and the atmosphere. So the leaf area also sets limits on transpiration and photosynthesis. For different vegetation types LAI can vary from less than 1 for deserts to over 6-8 for rain forests.

There are a variety of methods for measuring LAI. The most straightforward is to simply define an area on the ground, clip off all the leaves, and measure their area. Dividing the total area of all the leaves by the ground area gives LAI. The problem with the measurement of LAI is that they are difficult and time consuming to perform over large areas. Remote sensing provides a means to make repeatable, consistent measurements over large areas that can be related to LAI. Generally, LAI has been estimated from remotely sensed data by developing relationships between ground-measured LAI and spectral vegetation indices.

An example of the pattern of monthly LAI it is given for the year 2005 (for this index the patterns between years differ) (Fig.8).
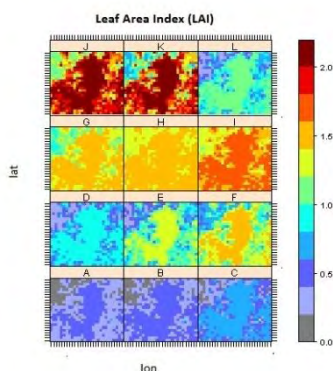

Fig. 8 The pattern of the leaf area index of every month for the year 2005
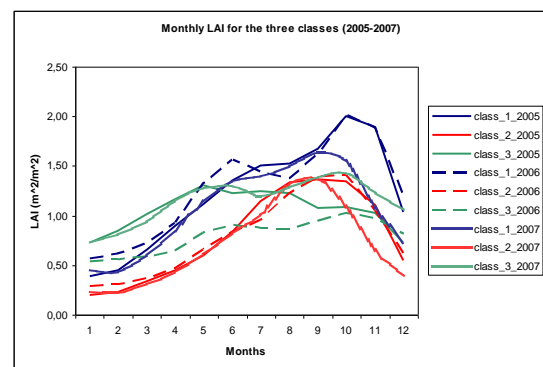

Fig.9 LAI distribution for the different classes and years (classes 1, 2 and 3 are for deciduous, tropical grassland and garden/parks, respectively)

From the data that we had, (as it shown at the Table 2), the parameter LAI depends on the time also. For obtaining the monthly values, we found the pixels which correspond to the three obtained classes (4.deciduous forest/ 11.Tropical grassland (C4)/ 12.Garden and parks) for all months of each year and then we computed the mean value of each class for every month.

Between the three classes of vegetation, there is a distinction between the types of deciduous forest, concerning their height, in overstory and understory. For the deciduous forest, there are appearing both of them, but for the other two categories we have only understory vegetation. Owing to that, our data provide information only for the total amount of LAI, we have done the separation by assuming that the values of overstory and understory appear the same weights:

$$\frac{LAI_u}{LAI_o} = \frac{1}{2} \quad \text{and} \quad 0.5 \cdot LAI_u + 0.5 \cdot LAI_o = LAI_i,$$

Where the LAI_i is the mean monthly value of each class, LAI_u is the understory leaf area index and the LAI_o overstory leaf area index. By applying the previous equation, we have taken the following of LAI for deciduous forest (Fig.10).
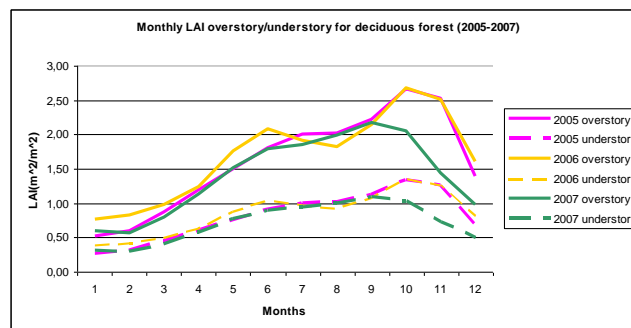

Fig. 10 The LAI distribution for overstory and understory for the first class (deciduous forest)

> ➤ Albedo (visible and near infrared)

Another important parameter to computed was the albedo, which is the fraction of the incident radiation that is reflected from the surface. Albedo plays a major role in the energy balance of the earth's surface, because it defines the rate of the absorbed portion of the incident solar radiation. The portion of solar radiation that is not reflected by the earth's surface is absorbed by the soil or the vegetation, which interacts with the incident radiation. The absorbed energy can increase the soil temperature or the rate of evapotranspiration from the surface of the soil/vegetation system. An amount also of the energy that is absorbed and transformed into heat is reradiated at a longer wavelength than the incoming radiation. The albedo value ranges from 0 to 1, with the minimum value corresponds to a blackbody (theoretical medium that absorbs all the incident radiation) while the maximum to an ideal reflector surface (absolute white surface).

In our case study, the values that were computed and derived from the data for the albedo were from two different bands, the visible broadband (0.4-0.7 μm) and near-infrared albedo (0.7-3.0 μm). At these two spectral regions is observed a marked difference of the reflectance of vegetation. Thus, the values depend on the nature of the interaction of solar radiation with the leaves at the given wavelength. The patterns that we had from the data for the year 2005 are shown at the next figure (Fig.11).
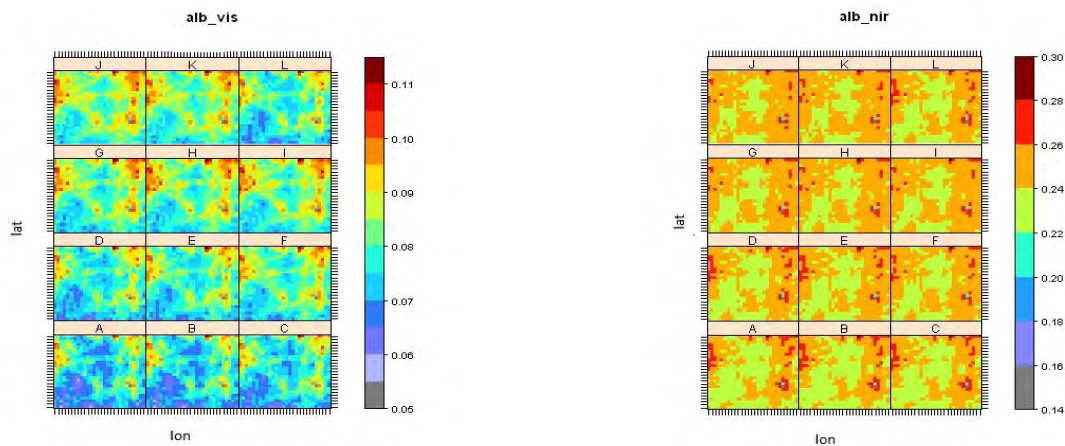
Fig. 11 The pattern of the visible and near-infrared albedo of every month for the year 2005

For obtaining the monthly values, was implemented same methodology with the LAI. There were found the pixels which correspond to the three obtained classes for all months of each year and then there was computed the mean value of each class for every month. The different values for the three classes and years 2005-2007 are presented at the following figure (Fig.12).
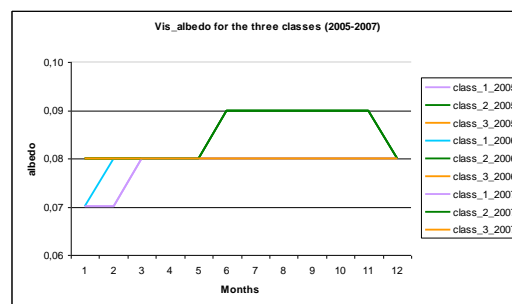

Fig. 12 The visible albedo distribution for the different classes and years (classes 1, 2 and 3 are for deciduous, tropical grassland and garden/parks, respectively)

The values for the visible albedo for each class present similar behaviour among the years. The only exception is the first class, which differs between 2005/2007 and 2006 only at the second month.

4.2 Pre-processing

4.2.1 Meteorological Data

The DHSVM requires a time series data for input. All the meteorological data that were used, have been taken from the ALMIP2 project. The atmospheric forcing data couldn't be used from the model at the MKS units, so it was necessary to be converted. For this reason, there were applied the following transformations:

- **Temperature**: The variable Tair is in °Kelvin, so we used the next formula to convert in °Celsius $T'_{air} = T_{air} - 273.15$

- **Wind**: From the forcing data there are the values of the eastward and northward wind components (Wind_E and Wind_N, respectively), and for finding the wind we compute the resultant by using the equation $Wind = \sqrt{(Wind\_E)^2 + (Wind\_N)^2}$.

- **Relative humidity**: For finding this ratio of the partial pressure of water vapor in the mixture to the saturated vapor pressure of water at a prescribed temperature, we used the formula $HR = \left(\dfrac{Q_{air} \cdot P_{Surf}}{Q_{air} \cdot P_{Sat} + 0.622 \cdot P_{Sat}}\right) \cdot 100 \, (\%)$, where

$$P_{Sat} = \exp\left[23.3265 - \left(\frac{3802.7}{T_{air}}\right) - \left(\frac{472.68}{T_{air}}\right)^2\right].$$

- **Precipitation**: The units have to be in $mm/30\min$ and there is the usage of the formula

$$R'_{a\inf} = R_{a\inf} \cdot \left(\frac{30 \cdot 60}{1000}\right) \cdot 1000.$$

For the shortwave radiation, longwave radiation, surface pressure and terrain (elevation), the values were taken without apply any modifications. Relatively the last parameter, the lapse rate temperature, there was assumed a constant decrease with the height that is equal to) 0.001°C/m.

4.2.2 Vegetation data

Between all the soil/vegetation parameters, one important variable that was used was the patch, because it was an index for the vegetation map that we had to extract. The spatial distribution patterns of vegetation are mostly identified as patch, which shows at every pixel the percent of the vegetation classification.

By taking the pattern for all the 12 months of every year (it was the same for the rest years), we noticed that the form was similar for the two months (Figure 13) and then we decided to take the maximum value of the same pixel for the different 12 months (Figure 14).
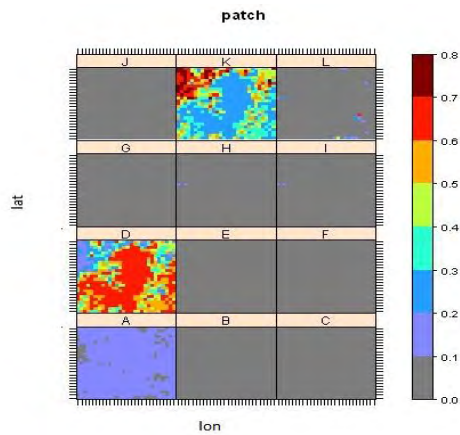
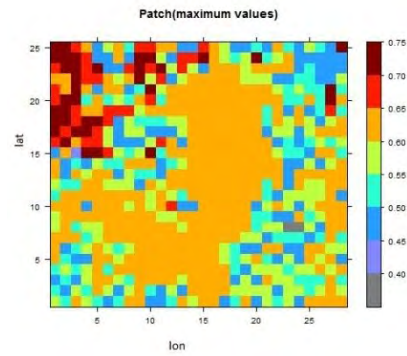Fig. 13 The pattern of the parameter patch for the 12 months

Fig. 14 The pattern of the parameter patch by selecting the maximum values of every month

Subsequently, we wanted to see in which land classes is referred the previous classification, because DHSVM uses only the dominant vegetation type of every grid cell. All grid cells with identical vegetation classifications are then assigned one set of vegetation dependent hydraulic parameters through a lookup table in the input file (Storck et al., 2000).

This classification is relied on 12 basic land classes (Table 4):

Land classification		
1. bare ground	5. conifer forest	9. irrigated crops
2. rocks	6. evergreen broadleaf trees	10. grassland (C3)
3. permanent snow	7. C3 crops	11. tropical grassland (C4)
4.deciduous forest	8. C4 crops	12. garden and parks

Tab. 4 Land classification

In our case study, by the identification of the maximum values (Fig.14) there are appearing only three from the previous classes, which are the following:

- 4.Deciduous forest
- 11.Tropical grassland (C4)
- 12.Garden and parks

By exporting these three classes from the patch parameter, then we took the next pattern (Fig.15).
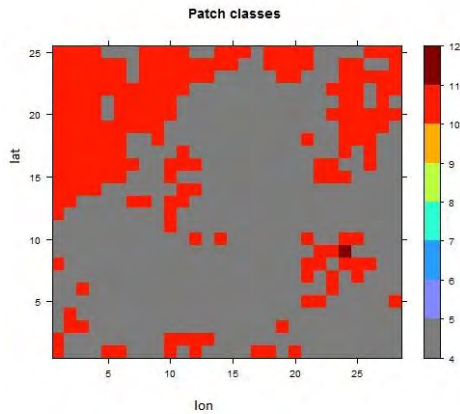
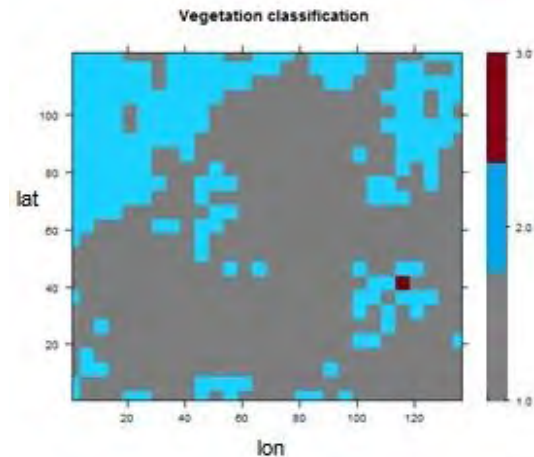Fig. 15 The pattern of the patch classification with the three classes

Fig. 16 Map for vegetation

Relying to the previous pattern, there was created the final map of vegetation (Fig.16) with three classes.

4.2.3 Soil data

The soil data is based on Food and Agriculture Organisation of the United Nations (FAO) (10 km spatial resolution) and includes sand and clay fractions. Each grid of 0.05^{o} is characterized by the percentage of 12 classes derived by the supervised classification of LANDSAT remote sensing images. Each of these soil classes is characterized by a given soil texture (coarse and fine fraction, the latter separated into clay, loam and sand) and soil depth. Texture indicates the relative content of particles of various sizes, such as sand, silt (loam) and clay in the soil. Texture influences the ease with which soil can be worked, the amount of water and air it holds, and the rate at which water can enter and move through soil.

In our case we used the USDA texture classification (Table 5), which was developed by the United States Department of Agriculture to provide indication of soils ability to support plant/crop growth and is based on relative proportions of sand, silt and clay.

Common names of soils (General texture)	Sand	Silt	Clay	Textural class
Sandy soils (Coarse texture)	86-100	0-14	0-10	Sand
	70-86	0-30	0-15	Loamy sand
Loamy soils (Moderately coarse texture)	50-70	0-50	0-20	Sandy loam
Loamy soils (Medium texture)	23-52	28-50	7-27	Loam
	20-50	74-88	0-27	Silty loam
	0-20	88-100	0-12	Silt
Loamy soils (Moderately fine texture)	20-45	15-52	27-40	Clay loam
	45-80	0-28	20-35	Sandy clay loam
	0-20	40-73	27-40	Silty clay loam
Clayey soils (Fine texture)	45-65	0-20	35-55	Sandy clay
	0-20	40-60	40-60	Silty clay
	0-45	0-40	40-100	Clay

Tab. 5 USDA textural classes of soils, based on the USDA particle-size classification

24 |

The parameters that we need to give is the fraction of sand and clay, as well as the soil depth. We wanted also to obtain the percentage of loam, which was taken easily from the following relationship:

$$loam = 1 - sand - clay$$

The initial patterns that result from the data are the following for the different types of soil texture for the year 2006 (the same pattern is used for years 2005 and 2007):
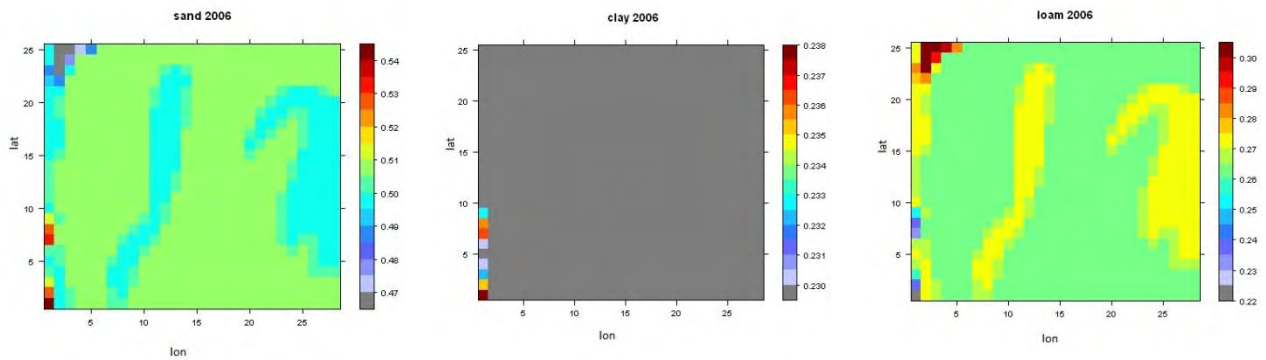

Fig. 17 The three maps which derive from the data for the year 2006 (for sand, clay and loam, respectively)

From the previous figure (Fig 17) it is easily clear, that the two main types of soil (sand and loam), appear exactly the same pattern. In contrary, clay present a constant value at the grid (equal to 0.23), with the difference only for longitude 1.475° and latitude from 8.975° up to 9.325° (the values range from 0.23 to 0.238).

The classification had to be based among the patterns of sand and loam. In our case study there are generated 3 soil classes (Table 6) and the selected map was the sand, for defining the appropriate intervals which gives the desired pattern. The values range from 0.47 up to 0.54. For having the final soil map (texture of every soil class in sand, clay and loam) have been extracted the same pixels from the clay and loam pattern.

Soil Classes	Interval of sand values
Class 1	0.4700 – 0.4960
Class 2	0.4961 – 0.5001
Class 3	0.5002 – 0.5402

Tab. 6 The three classes and the values of sand, where is based the classification

The final map for the soil after the classification is shown at the next figure (Fig. 18).
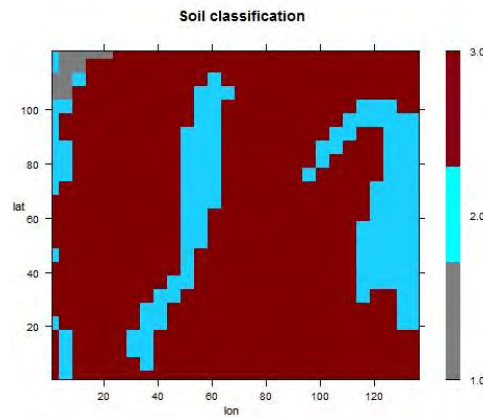
Fig. 18 The final map of the soil classification

For finding the texture of every soil class and ranking our three different type soils, according to the USDA classification, we had to compute the mean values of the pixels, which were corresponded to every class. Except for the sand, we had to obtain first the same pattern for the clay and loam, thereafter to extract the suitable pixels that represent every class and then take the mean value separately for each class.

The final texture of that were obtained, is shown at the next table:

Soil Classes	Percentage of every class(%)		
	Sand	Clay	Loam
Class 1	0.478	0.230	0.291
Class 2	0.499	0.230	0.270
Class 3	0.509	0.230	0.260

Tab. 7 Percentage of sand, clay and loam for the three classes

From the values that were found (Table 7), according to the texture triangle (Figure 19), class 1 corresponds to Loam (Lo), while classes 2 and 3 are characterized as Sand_Clay_Loam (SaClLo).
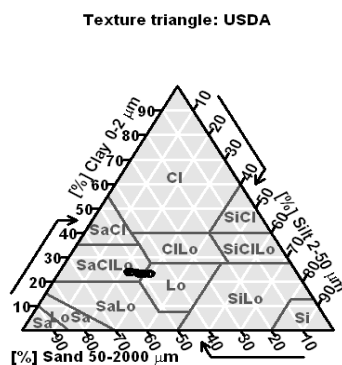
(a)
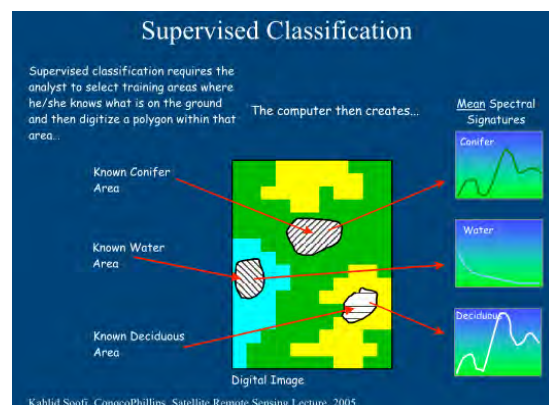
(b)

Fig. 19 Triangular diagram of the basic soil textural classes according to USDA particle sizes (a) and the supervised classification (b)

Another map that is need by the model as input data is the soil depth map. It is also generated from the data and the pattern is shown at the next figure (Fig. 20).The soil depth varies from 1.7 up to 2.55 m.
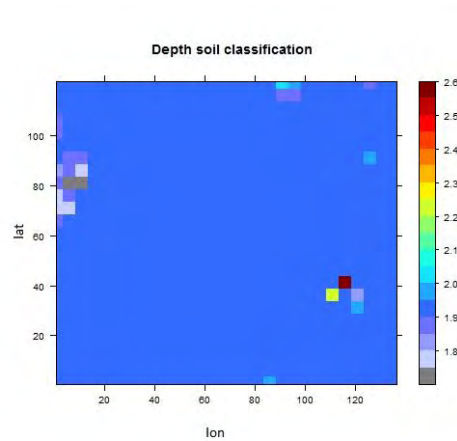
Fig. 20 The soil depth map

4.2.4 Digital Elevation Model (DEM)

The basis of the DHSVM model is the map with the elevation because it provides the topographic controls required by the model calculations. The grid that we have is shown at the following figure (Fig.21).
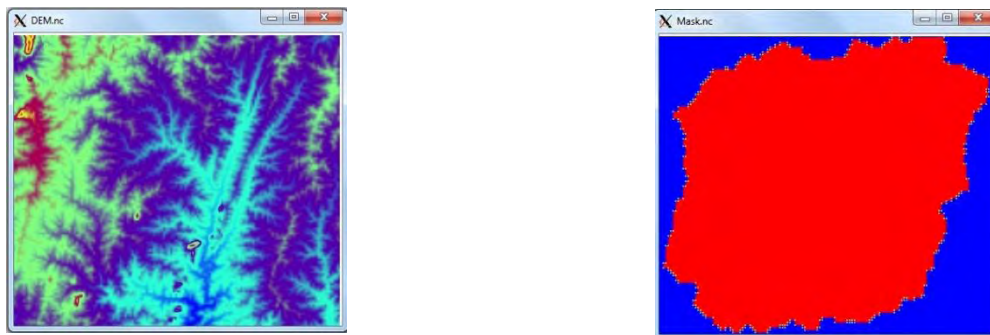
Fig. 21 Maps for DEM and Mask, respectively

4.2.5 Basin mask

The maps that created previously cover our basin, but they don't give exactly the shape of our basin. For this reason it is needed the creation of the mask, to provide the analysis domain for the model calculations. The mask indicates to the model which pixels have to be taken into account for carrying out the numerical simulations. The DHSVM only simulates hydrologic processes on cells within the masks. Although the entire grid contains 16456 pixels (136 x 121), the number of active pixels is 11788 (Fig. 21).

27 |

4.2.6 Stream input

DHSVM needs three different files for the stream channels: class, network and map. The first two contain information about the routing and the segments of the stream (related to each stream order). These include information about the hydraulic width, which calculates the volume of storage in the stream, the depth of the stream channel, Manning's coefficient, slope of the channel segment and identification of the segment in which goes the flow. The map file links the previous physical stream data to cell locations.

4.2.7 Initial model state

The last of the input files is that one which contains the initial values. It is very useful, because every time that we want to do a new simulation, it allows the model to restart with exactly the same initial conditions. There have been created four different files for this purpose. The channel state and the interception file, contain the amount of water in each channel segment and the interception variables (rain and snow interception storage for the overstory and understory, as well as the temporary interception storage for the overstory), respectively. These values were assumed that are equal to zero.

The other two files are the soil and snow state. Their values are presented in the next table (Table 8).

Parameter	Soil state		
	Description	Units	Value
Soil.Moist	Volumetric soil moisture content for each layer	-	0.02 0.05 0.05 0.05
Soil.TSurf	Temperature at soil surface	°C	26
Soil.Temp	Soil temperature for each root zone layer	°C	24 22 20 20
Soil.Qst	Ground heat storage	J	0
Soil.Runoff	Surface ponding	m	0.01
	Snow state		
Snow.HasSnow	Whether snow is present (1) or absent (0)	-	0
Snow.LastSnow	Number of days since last snowfall	-	300
Snow.Swq	Snow water equivalent	m	0
Snow.PackWater	Liquid water content of bottom layer of snow pack	m	0
Snow.TPack	Temperature of bottom layer of snow pack	°C	26
Snow.SurfWater	Liquid water content of top layer of snow pack	M	0
Snow.TSurf	Temperature of top layer of snow pack	°C	26
Snow.ColdContent	Cold content of snow pack	J	0

Tab. 8 Soil and snow initial state parameters

4.3 Configuration File

The DHSVM configuration file relays all the input variables to the model. It contains information on the model settings, constant parameters (ground and snow roughness, rain and snow threshold, height of all the meteorological observations, e.t.c), path names of the files and maps, soil parameters, vegetation parameters and output options (maps with the results parameters that have to be created).
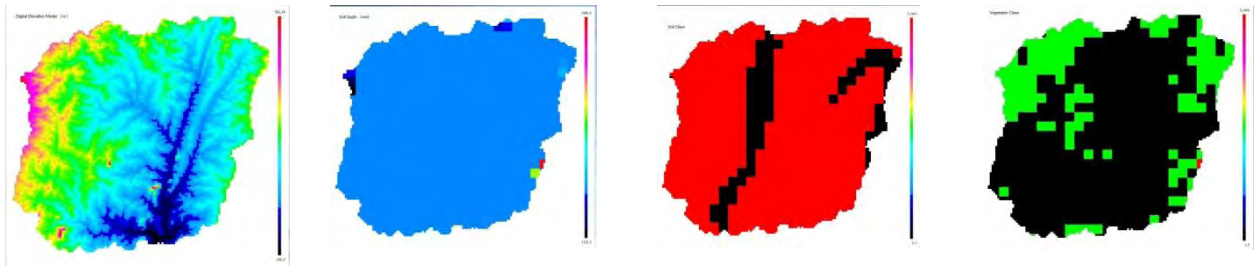
Fig. 22 The final maps for DEM, soil depth, soil and vegetation, respectively

These parameters of the model stay constant to the time and space during model calculations. The needed parameters are roughness (ground and snow), threshold (snow and rain), snow water capacity, reference height, leaf area index multiplier (rain and snow), minimum intercepted snow, lapse rate of temperature and precipitation.

The roughness has to do with the height above the ground, in which the mean wind speed becomes zero. Is a measure of the variability of surface microtopographic features and it influences the movement of air across the snow surface and resulting transfers of energy (Fassnacht et al., 2009). The rain and snow threshold are the minimum values of temperature, where both of these situations can occur. This rain/ snow transition occurs when the phase of precipitation changes from rain to snow or snow to rain. At a fixed location, this occurs as different air mass characteristics move across the site, which produces changes in phase. This is not appearing the same in a mountainous basin, because happens something more complicated than lateral air-mass movement, because the rain/snow transition may occur rapidly during an event as a combined function of changes in elevation and air mass characteristics. These temperatures are not exactly for all the cases exactly at 0°C, but depend on surface temperature, the dew point and the wet bulb temperature (Marks et al., 2012).

The liquid water capacity of snow as well as the minimum intercepted snow, do not have important effect in our study. The water capacity of snow depends on many factors, such as the topography, ice layer characteristics and snow density. The second parameter is used at the snowpack model. A reference value that can be derived from Storck (2000), is that the minimum amount of intercepted snow that can be melted or sublimated off the canopy is about 0.005m.

Another component that is presented at the configuration file, is the reference height in which the atmospheric observations were taken. Usually, it is taken some meters more than the highest canopy height. In our case, although we have not tall enough trees, we preferred to take this reference height enough meters more than the canopy. The model uses also the LAI multiplier for modeling the maximum interception storage capacity. A default value is taken equal to 0.0001 (Wigmosta et al., 1994).

For the lapse rate temperature, that is the rate of decrease with the height. The measurable rapes rate is affected by the moisture content of the air (humidity). It was found that dry lapse rate is about 0.010°C/m (for calculate temperature changes in air not at 100% of relative humidity), while a wet lapse rate is about 0.0055°C/m (for saturated air). High resolution gridding of climate data, for applications to hydrological modeling, rely on assumption that there is a constant lapse rate between 0.0060 and 0.0065°C/m. The second value has been selected for our case (Minder et al., 2009). The use of these values is probably attributable in part to various sources that are referred to as mean free atmosphere lapse rates in this range. Except of the temperature lapse rate there is also needed for the precipitation. For simplifications, we assumed that is zero.

Despite the constants, our model requires numerous soil input parameters for each soil type and for every horizon. All these soil and vegetation parameters have to complete for every soil and vegetation classification.

4.3.1 Soil parameters

DHSVM requires many soil input parameters, separately for every soil type and for every horizon of each type. One parameter is the saturated hydraulic conductivity that represents the volume of the unit water that flows through the saturated soil, in a given unit of time. It is one of the most important soil properties that control water infiltration and surface runoff. It depends on soil texture and structure and therefore can vary widely in space. Hydraulic conductivity also shows a temporal variability that depends on different interrelated factors, including soil physical and chemical characteristics affecting aggregate stability and climate dynamics. Also, it was assumed that the lateral hydraulic conductivity for each soil decrease exponentially with depth, for the calculation of the rate of the saturated subsurface flow. The values are between 1 and 9, where in our case has been selected the first value.

Infiltration, the process of water entry into the soil through the soil surface, is generally the main loss mechanism in the generation of overland flow, and its determination has important applications. Several models represent local infiltration into vertically homogeneous soils fairly accurately. However, natural soil profiles are typically not homogeneous in the vertical direction. Often a thin upper layer of lower permeability develops because of the formation of a crust on the surface of bare soils or the soil permeability decreases with depth as in tilled soils with vegetation. Infiltration occurs preferentially in areas where the permeability of the terrain, associated with other factors, allows the rapid penetration of surface waters. Part of this water percolates through the non-saturated zone of the ground and on reaching the water table, recharges the aquifer. The rate at which water moves into the soil surface is the infiltration capacity. When the infiltration rate for a soil has reached the maximum value, then no more infiltration can occur and surface runoff or ponding will happen. This maximum rate depends on many soil characteristics, such as texture and structure.

Some other parameters that are required are the capillary drive and bubbling pressure. The capillary suction measures the adhesive forces that tie water molecules to soil particles and the cohesive forces that tie water particles to each other. In addition to, when there is a

decrease of the water content, the capillary suction increases and depends on components like the soil texture and soil moisture. Concerning the second parameter, it is referred to the air pressure that is required to force air through a porous medium (is a function of the maximum pore size forming a continuous network of flow channels within the medium) (Brooks and Coley, 1964). This pressure is needed for the model when calculating desorption in the model, which is a part of the movement of unsaturated soil moisture. This parameter, like some others, has been found with the aid of some functions that are describing thereafter.

Of course, one more significant parameter is the soil porosity, which is a measure of the void spaces in a porous medium and it is defined as the fraction of the volume of voids over the total volume (Bal et al., 2012). It is very important to hydrologic calculations, because controls the total amount of water stored and transmitted. One parameter that is interdependent from the porosity is the bulk density, which expresses the weight of a unit volume of dry soil that includes the volume of solids and pore space. Another volume that is necessary is the one from the various sizes of pores and is known as pore size distribution. Our model uses the pore size distribution when modeling the percolation of water through the soil column.

Again with the aid of some functions there have been computed also the field capacity and the wilting point. The first one is the water content of the soil where all free water has been drained from the soil through gravity and occurs at soil suctions between 5-30kPa, depending on the soil characteristics. While the other parameter is the soil moisture content (minimum) at which the plant will wilt and die (or at which most plants cannot obtain sufficient water to prevent permanent tissue damage).

Except of the previous parameters, there are needed some additional that have to do with the heat, the thermal conductivity and the thermal capacity. They play an important role in the surface-energy partitioning, resulting temperature distribution, moisture flow and consequently form the soil and near ground atmosphere microclimate for plant growth (Lipiec J et al., 2007). The first one express the ability to transmit heat, mainly through transmission and is defined as the quantity of heat that flows through a unit area in a unit time under a unit temperature gradient. Moreover, for finding this component was used the following equation from Bowling and Lettenmaier (1997):

$$TC = \frac{S \cdot TC_{quartz} - C \cdot TC_{clay}}{S + C}$$

Where S is the percent in sand from our texture identification, C is the percent in clay, the thermal conductivity of quartz is $TC_{quartz} = 8.8 Wm^{-1}K^{-1}$, and the thermal conductivity of the clay is $TC_{clay} = 2.9 Wm^{-1}K^{-1}$. The thermal capacity is the change in heat content of a unit bulk volume of soil per unit change in temperature. These thermal properties are significantly influenced by variable soil water content, bulk density, temperature and by stable mineralogical composition and organic matter content.

Another parameter that controls the surface radiation budget and is needed from the model, is the surface albedo, which is the fraction of the incident radiation that is reflected

from the surface. It defines the rate of the absorbed portion of the incident solar radiation and the part that is not reflected is absorbed by soil or vegetation. This energy can increase the soil temperature or the rate of evapotranspiration. It varies spatially and evolves seasonally based on solar illumination changes, vegetation growth and human activities (cutting/planting forests) (Tao He et al., 2012). It can have a value of 0.1 for dark surfaces and 0.5 for lighter surfaces.

All the values of the previous parameters are presented at the next table (where some of them derived from bibliography, while some others were calculated by a way that is describing afterwards), for each of the three different soils according to our classification:

Soil parameters						
Parameter	**Description**	**unit**	**Soil 1 (Loam)**	**Soil 2 (SaClLo_1)**	**Soil 3 (SaClLo_2)**	
Lateral conductivity	lateral saturated hydraulic conductivity	m/s	0.0001	0.0001	0.0001	
Exponential decrease	exponent for change of lateral conductivity with depth	-	1.0	1.0	1.0	
Maximum infiltration	maximum infiltration rate	m/s	3.2e-5	6.0e-5	6.0e-5	
Surface albedo	albedo of the bare soil surface	m/s	0.2	0.2	0.2	
Porosity	porosity of each soil layer	-	0.4464	0.4435	0.4422	
Pore size distribution	% of bulk volume of various sizes of soil pores for each soil layer	-	0.3965	0.3816	0.3756	
Bubbling pressure	air entry value for each soil layer	m	0.5747	0.5235	0.5025	
Field capacity	the water content of the soil where all free water has been drained from the soil through gravity	-	0.4018	0.3992	0.3980	
Wilting point	water retained for each soil layer	-	0.0663	0.0600	0.0656	
Bulk density	the weight of a unit volume of dry soil, which includes the volume of solids and pore space	Kg/m^3	1494.72	1502.55	1506.06	
Vertical conductivity	vertical saturated hydraulic conductivity for each soil layer	m/s	1.218e-6	1.3287e-6	1.375e-6	
Thermal conductivity	the heat flow through an area of the square metre of soil subjected to a temperature gradient of 1°C per meter	W/m°C	6.886	6.941	6.964	
Thermal capacity	the heat required to raise the temperature of one cubic meter of the soil by 1°C, without change of moisture content	$J/m^3°C$	2.2e6	2.2e6	2.2e6	
Capillary drive	a gradient at the wetting front	m	0.11	0.263	0.263	
Mannings n	Manning's roughness coefficient	-	0.1	0.1	0.1	

Tab. 9 Input values of the soil parameters

To specify some of the soil hydraulic characteristics or properties, there were developed many indirect methods (Rawls et al., 1991, van Genuchten and Leiih, 1992), which use more easily measurable soil properties (particle size distribution, bulk density and organic matter content), for predicting the water retention curve. These models are referred to as pedotransfer functions (PTFs) (Bouma, 1989). Moreover, it was found that by using them, there is reflected better their spatial variability. (Manus C. et al., 2009).

The PTF's could be divided into three groups (Cornelis et al., 2001). The first one approaches to estimate soil water contents at particular suction head values by multiple linear regression (Rawls and Brakensiek, 1982) and/or using artificial neural networks (Minasny and McBratney, 2002). The second one predicts the parameters of a closed-form analytical equations, like those by Brooks and Corey (1964), Rawls and Brakensiek (1985) or van Genuchten (1980). This is again achieved by multiple linear regression or artificial neural

networks (Pachepsky et al., 1996, Schaap et al., 1998). The last group of PTFs is based on a physical-conceptual approach of the water retention phenomena and uses fractal mathematics and scaled similarities. Commonly, either the regression or the artificial neural networks have been used to find the parameters of pedotransfer functions. These methods can be called parametric. In our case study, we used a specific software to obtain the estimation of five parameters (by using the equations of van Genuchten) of water retention and the saturated hydraulic conductivity.

This program uses the hierarchical pedotransfer functions (PTFs) for the estimation of water retention, the saturated and unsaturated hydraulic conductivity, with the knowledge of which there have been estimated the van Genuchten parameters. It is about statistical regressions and one general remark concerning PTFs, is that their use has many limitations, because there are many cases where one or several input variables needed for a PTF are not available. For this reason, these values arose with the

use of the HYDRUS modelling software, which is used for analysis of water flow, heat and solute transport in soils, as well as for problems that demonstrate infiltration, evaporation and percolation through soils of different textures. It is supported by an interactive graphics-based interface for data pre-processing, discretization of the soil profile and graphic representation of the results. It is based on ROSETTA, which is a computer program for estimating soil hydraulic parameters with hierarchical pedotransfer functions (Schaap M. et al., 2001) and gives the highest correlation among all PTFs.

The HYDRUS software permits the use of five different analytical models for the hydraulic properties (Brooks and Corey, 1964; van Genuchten, 1980; Vogel and Cislerova, 1988; Kosugi, 1996 and Durner, 1994). As it was referred previously, the parameters were taken from the van Genuchten (1980) model, which used the statistical pore-size distribution model of Mualem (1976) to obtain a predictive equation for the unsaturated hydraulic conductivity function in terms of soil water retention parameters.

The dimensionless water content is defined as:

$$\Theta = \frac{\theta - \theta_r}{\theta_s - \theta_r}$$

where h is the pressure head and r and s indicate residual and saturated values of the soil water content (θ) ($cm^3 \cdot cm^{-3}$), respectively. (Van Genuchten M., 1980).

Moreover, there is also $\Theta = \left[\dfrac{1}{1+(a \cdot h)^n}\right]^m$. From these two equations, the retention function is given by:

$$\theta(h) = \theta_r + \frac{\theta_s - \theta_r}{[1+(a \cdot h)^n]^{(1-1/n)}}$$

where $\theta(h)$ is the measured volumetric water content ($cm^3 \cdot cm^{-3}$) at the suction h (is in cm and is taking positive for increasing suctions).

The parameter α is related to the inverse of the air entry suction and it is positive (cm^{-1}). Finally, n is a measure of the pore-size distribution and takes values greater than 1.

The unsaturated hydraulic conductivity is $K(h) = K_s S_e^L \left[1 - (1 - S_e^{1/m})^m \right]^2$, where $m = 1 - 1/n$ with n>1.

Also, the effective saturation is computed by $S_e = \dfrac{\theta(h) - \theta_r}{\theta_s - \theta_r}$.

At the previous relation factor L is an empirical parameter that is normally assumed to be 0.5 (Mualem, 1976). The above equations contain five independent parameters: residual water content θ_r, saturated water content θ_s, the factor α which is related to the inverse of the air entry suction, the factor n which is a measure of pore-size distribution and the saturated hydraulic conductivity K_s .The values for the three soil classes are presented at the next table (Table 10).

Soil Types	Fitted parameters from pedotransfer functions				
	θ_r (cm^3/ cm^3)	θ_s(cm^3/ cm^3)	α (cm^{-1})	n(-)	K_s (cm.day^{-1})
Loam	0.0663	0.4018	0.0174	1.3965	10.53
SaClLo_1	0.0600	0.3992	0.0191	1.3816	11.48
SaClLo_2	0.0656	0.3980	0.0199	1.3756	11.88

Tab. 10 The five fitted parameters that derived from the solution of the pedotransfer functions

The previous parameters were not the required from the model, except of the hydraulic conductivity K_s. But from them have been resulted the parameters:

- *porosity:* it was computed from the equation $\eta = \dfrac{\theta_s}{0.9}$, where θ_s is the saturated water content

- *bubbling pressure head:* it was found from $h_d = \dfrac{1}{a}$, where α is a factor related to the inverse of the air entry suction.

- *pore size distribution:* was carried out from the relation $\lambda = n - 1$, where n is a measure of pore-size distribution.

- *bulk density:* it was used the equation $\rho_{bulk} = (1 - \eta) \cdot \rho_{particle}$, where η is the porosity and from bibliography for our case study we assumed that the particle density $\rho_{particle}$ is equal to $2.7 \cdot 10^3 \, kg/m^3$.

Finally, with the use of all previous equations we take the next table for every soil type:

Soil Types	Parameters of DHSVM model				
	h_d (m)	λ (-)	ρ_{bulk}(kg/m^3)	η(-)	K_s (m/s)
Loam	0.5747	0.3965	1494.72	0.4464	1.2180e-6
SaClLo_1	0.5235	0.3816	1502.55	0.4435	1.3287e-6
SaClLo_2	0.5025	0.3756	1506.06	0.4422	1.3750e-6

Tab. 11 Some factors that were computed with the help of the previous fitted parameters

Moreover, for the field capacity and the wilting point, another assumption that we have done was to take them directly from the values that were derived from the fitted parameters from the pedotransfer functions, which are closed to these values. So, respectively we take the saturated water content and the residual water content.

4.3.2 Vegetation parameters

DHSVM model requires also a great number of input parameters that are relevant to describe the vegetation, for each cover type (Table 12). Moreover, something which derives from the structure of the model, is the presence of overstory and understory vegetations. When we have both of them, the model requires a greater amount of parameters for the simulations.

The fractional coverage is the fraction of the total area that is occupied by the overstory and is used when computing the maximum storage interception capacity for the canopy, as well as the longwave and shortwave radiation budgets. Also, concerning the height of the tree, the model requires an input for the fractional proportion that the trunk space exhibits in comparison to the entire tree height, for computing the aerodynamic resistance. For deciduous trees, in addition to wind speed dependence, the aerodynamic resistance varies during the growing season as the canopy develops and for fast growing trees, as the height increases. It is very important for the estimation of interception loss from a saturated canopy, when the canopy resistance is zero and the aerodynamic resistance is the only one constraining evaporation (Hall R., 2002).

The aerodynamic attenuation parameter is a dimensionless coefficient that is used for calculating the exponential wind profile through the overstory canopy (Wigmosta et al., 1994). There is not only needed the aerodynamic, but also the radiation attenuation. It is about again for a dimensionless coefficient that is used for the calculation of the fraction of the shortwave radiation transmitted by the overstory, using the Beer's law (Wigmosta et al., 1994). For finding the precise value, it is necessary of having some information concerning the distribution of the leaves (the angle in relation to the ground and the azimuth angle with respect to direction around the branch of the tree). In our case there have been missing these values and this parameter was based again to literature.

Concerning the parameters that are relevant with the snow, there is needed from the model to define the maximum value of the snow interception capacity, which depends on the branch strength under stress and the shape of the canopy as opposed to the leaf shape, which is the most important factor for the rainfall interception. The snow will stay to the branches up to the time that the snow begins to melt or the strength of the branch can no longer stand the weight of the snow. Moreover, there has to be obtained the value of canopy ability to intercept snowfall and prevent it from reaching the ground (is dependent on temperature and wind speed) and is called snow interception efficiency. Except of this one, another parameter is the maximum release drip ratio, which is the ratio of snow in the canopy that falls as snow (mass release) to the snow that melts off of the leaves (meltwater drip). Storck et al. (2002) found that a drip ratio of 0.4 was appropriate. The same default value has been selected in our case study.

The impervious fraction is the amount of impervious surface area present within the grid cell. Impervious surfaces are those that water cannot infiltrate and are primarily associated with transportation (such as streets, highways, sidewalks) (Yuan F. et al., 2007). Here, it was assumed to have an impervious fraction equal to zero. Another necessary parameter is the height for each vegetation layer (overstory and understory). The last decade there have

been noticed significant advances in the development of active sensor technologies that made it possible to obtain consistent and reliable estimates of vertical structural metrics. These advances include sensors such as Light Detection and Ranging (LIDAR), as well as microwave scatterometers for a highly accuracy and spatial resolution estimation of forest vertical structure and vegetation height (Kellndorfer J. et al., 2004). In our study, there was lack of this information, so it was assumed for the deciduous forest the height for the overstory is 6 m, while for understory 50 cm. For the second class of our classification a value of 30 cm has been selected.

Any natural surface partitions the net supply of radiative energy into sensible and latent heat flux. In the case of vegetation the key factor in this partitioning is the stomatal behaviour (Lhomme J et al., 1998). These parameters operate as a measurement of the plant's ability to control transpiration. Among numerous approaches allowing the calculation of the partitioning over vegetation, is the model that formulated by Penman-Monteith which has acquired a wide acceptance by its simplicity and its performance. In this approach the behaviour of stomata is represented by a canopy stomatal resistance assumed to be comparable with that of a single leaf and influenced by the same factors.

Another parameter is the moisture threshold, when soil moisture falls below a certain water content then transpiration is restricted. Except of this, there is also needed the vapor pressure deficit, where at higher values vegetation (plants) require more effort to carry water from the roots to the leaves. At a high enough of this pressure, stomatal closure will occur. The values of this parameter are necessary for the computation of the canopy resistance (Wigmosta et al., 1994).

Three last parameters that are required are the fraction of shortwave radiation that is photosynthetically active for every canopy layer (Rpc), the depth of the root zones, as well as the overstory and understory root fraction. The first one, according again to Wigmosta (1994) is the light level where the stomatal resistance is twice of the minimum stomatal resistance, while the second one is the depth of the soil layers. DHSVM need also information concerning the fraction of roots in each root zone for every canopy layer. The values that were chosen rely on the assumption that upper layers contain more roots than the deeper soil layers.

			Vegetation parameters					
Parameter	Description	unit	Vegetation 1 (Deciduous forest)		Vegetation 2 (Tropical grassland (C4))		Vegetation 3 (Garden and parks)	
			overstory	understory	overstory	understory	overstory	understory
Overstory /Understory presence	whether an overstory and/ or understory is present	-	TRUE	TRUE	FALSE	TRUE	FALSE	FALSE
Fractional coverage	the fraction of total area occupied by the overstory	-	0.9		-		-	
Trunk space	distance from the ground surface to the start of the crown	m	0.4		-		-	
Aerodynamic attenuation	canopy attenuation coefficient for the wind profile	-	3.5		-		-	
Radiation attenuation	radiation attenuation of the overstory	-	0.5		-		-	
Maximum snow int int capaci	maximum snow interception	m (of	0.04		-		-	

Parameter	Description	Unit					
	capacity for the overstory	water equivalent)					
Max release drip ratio	ratio of mass release to melt water drip from intercepted snow	-	0.4		-		-
Snow Iterception eff	percentage of snowfall intercepted until the maximum snow interception capacity has been met	-	0.6		-		-
Impervious fraction	impervious fraction of vegetation type	-	0.0		0.0		0.0
Height	height of each vegetation layer	m	6.0	0.5	-	0.3	-
Maximum resistance	maximum stomatal resistance for each vegetation layer	s/m	6000	4500	-	3000	-
Minimum resistance	Minimum stomatal resistance for each vegetation layer	s/m	126.0031	100.0	-	116.4524	71.70834
Moisture threshold	soil moisture threshold above which soil moisture does not restrict transpiration for each vegetation layer	-	0.30	0.10	-	0.33	-
Vapor pressure deficit	vapor pressure deficit threshold above which stomatal closure occurs for each vegetation layer	Pa	2500	3000	-	2000	-
Rpc	fraction of shortwave radiation that is photosynthetically active for each layer	-	0.108	0.108	-	0.108	-
Number of root zones	number of rooting zones	-	3		3		3
Root zones depths	thickness of soil layers	m	0.5 0.5 0.4		0.5 0.5 0.4		0.4 0.3 0.3
Overstory root fraction	fraction of the roots of the overstory in each root zone layer	-	0.5 0.5 0.0		-		-
Understory root fraction	fraction of the roots of the understory in each root zone layer	-	0.6 0.4 0.0		0.6 0.4 0.0		-
Overstory monthly LAI	overstory leaf area index for each of the 12 months	-	not presented here the values (see chapter 4.2.2)		-		-
Understory monthly LAI	understory leaf area index for each of the 12 months	-	not presented here the values (see chapter 4.2.2)		not presented here the values (see chapter 4.2.2)		-
Overstory monthly alb	overstory albedo for each vegetation for each of the 12 months	-	not presented here the values (see chapter 4.2.2)		-		-
Understory monthly alb	understory albedo for each vegetation for each of the 12 months	-	not presented here the values (see chapter 4.2.2)		not presented here the values (see chapter 4.2.2)		-

Tab. 12 The values of the vegetation parameters

5. Output data-First results

After having describe all the land surface characteristics data and the meteorological time series, the DHSVM model during the simulation tracks hydrological variables and fluxes, like snow water equivalent, depth to saturation and soil moisture in two subsurface zones and moisture intercepted on the vegetation as snow or liquid (Storck et al., 1998). The goal of the hydrologic modelling by using a distributed model like this is to represent the physical processes that occur within our basin, influenced by both atmospheric forcing and basin physical characteristics, and to produce a prediction of runoff rates and volume. At this case study, there has been a focus at the streamflow because of the existence of validation data in two sites.
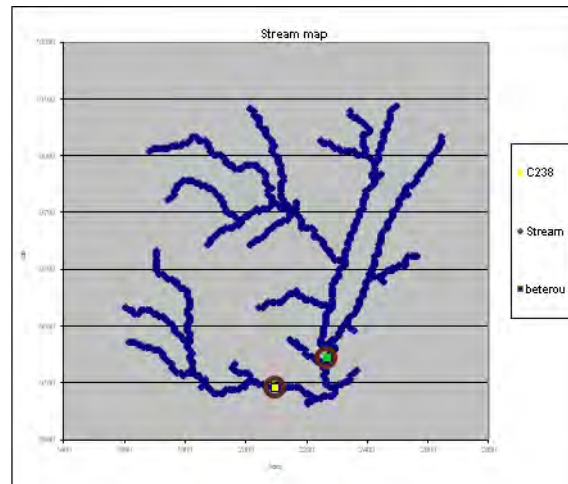
Fig. 23 The two sites where observed data for streamflow were available

5.1 Un-calibrated simulations

The two locations where observed data of streamflow were available, are the Beterou and the C238 (Fig. 23). Their annual streamflow for the year 2005 is presented at the next figure (Fig. 24).
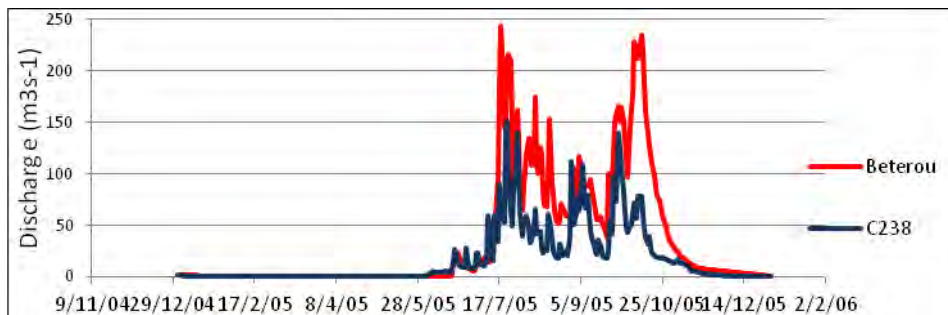

Fig. 24 Annual streamflow for the year 2005 for the two sites (Beterou and C238)

The precipitation in our case study was 1048 mm (Fig.25). Most of the rains fall during summer up to September. In this area, during this period is appearing the 60% of the rainfall and rivers dry up from mid-December to March (Séguis et al.,2011). Concerning evapotranspiration, it was found by the model results to be about 800mm (Fig 26).
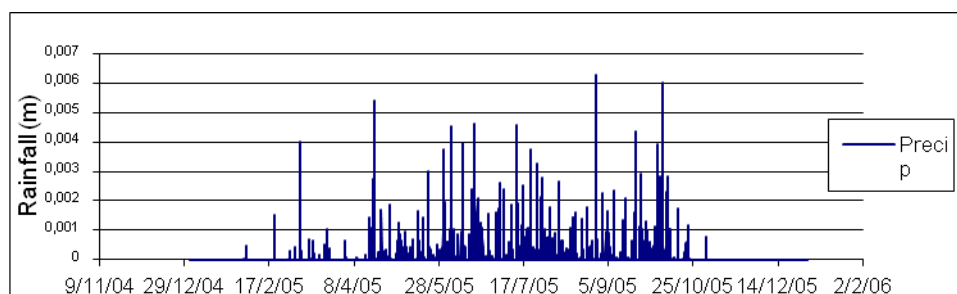

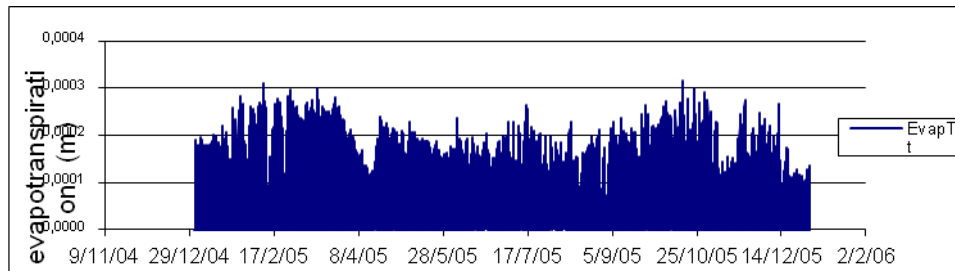Fig. 25 Precipitation for the whole basin for the year 2005

Fig. 26 Evapotranspiration for the whole basin the simulation year 2005

From the results that were derived from the model simulations (refer to the whole basin), some variables present the expected profile, while some others not. For example, one important variable is the soil moisture, which is increasing during the rainfall period (reaching the saturation) and after is decreasing again (Fig. 27). For the soil moisture, the results are really good, except of the fact that it remains stable at the values close to saturation for so much time. We expected not to be the soil saturated for too much time. This profile is referred only to the upper soil layer. In contrast, something similar it doesn't appear at the deeper layer and it is something that could be explained due to percolation.

In addition to, there have been also and some others variables, which have computed by the model (have to do with the radiation and the heat flux) where there are appearing zero values. More specifically, the net radiation (which is the sum of the latent, sensible and ground flux), is always zero. At this point, we didn't achieve to understand why after the model computations we are obtaining only zero values.
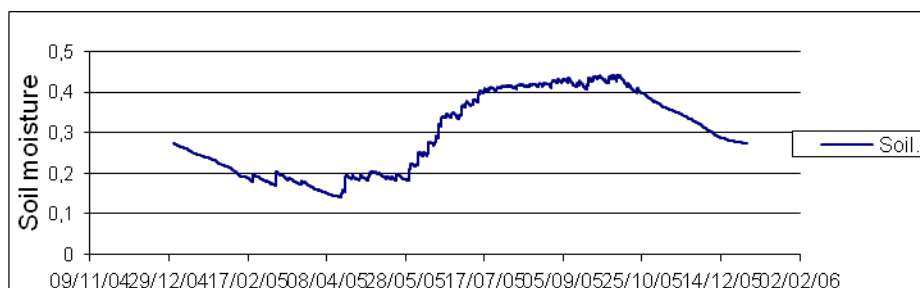

Fig. 27 Profile of the soil moisture (at the upper layer) for the simulation year 2005

For every simulation that has been performed, we have derived some results that had to do with the water mass balance in our basin. These results has to do for example with the inflow (precipitation), the evapotranspiration, the amount of water storage (which is the difference between the end of the run storage and the initial storage) as well as with the amount of the soil moisture. Another problem that arose, was the value of the mass error. It was not negligible, because it was more than 100mm and in some cases about 195mm. It indicates that the catchment water balance is not well simulated.

Having the data to compare with the simulated outputs that gives the DHSVM model, there has been made an effort to calibrate the model. The calibration of physically based distributed models requires particular attention because of the number of parameters involved. For this reason, and because of our focus to discharge, there was a priority to select and change some of the factors that affect the runoff generation, which is caused by

39 |

different physical mechanisms (for example Hortonian overland flow and infiltration excess runoff). From the output of the model we are taking information for the profile of the infiltration excess, which is a factor that gives the dynamic of occurring runoff out of our basin (Fig. 28). Apart from this, at the soil parameters that have been described previously, there is also the value of the maximum infiltration, which plays the role of the threshold, above which if we have rainfall then we have runoff.
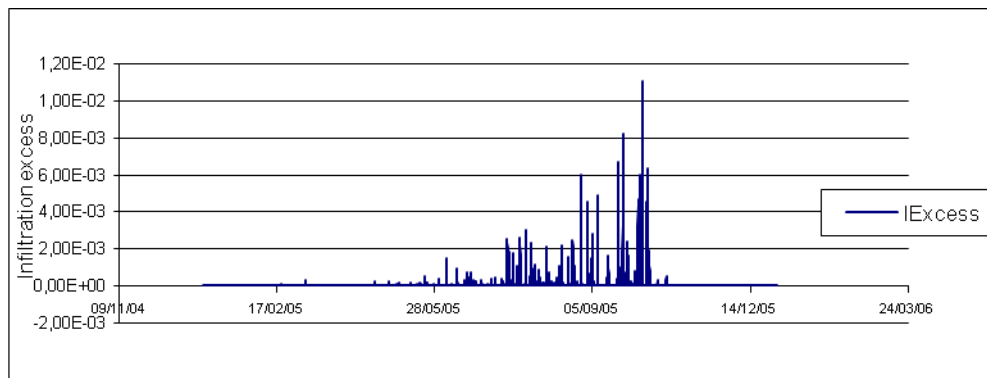

Fig. 28 Profile of the infiltration excess for the simulation year 2005

5.2 Sensitivity Analysis

The purpose of the sensitivity analysis is to determine which parameters have the greatest impact on simulation output. In our case study, due to lack of time, has been made an effort of realising a sensitivity analysis of some parameters, by changing the reference values systematically one at a time. Up to this time, this analysis has been done only by changing some soil parameters, as well as parameters that have to do with the stream. Before all these simulations that have been carried out, it is worth mentioning that the initial conditions didn't preserved, but have been changed and the new one that have been taken, were the values of the last day of the previous simulation.

One parameter that has been selected was the Manning coefficient of the soil as well as of the stream. For the first one, have been selected values that vary from 0.05 up to 0.2, while for the second one range between 0.02 and 0.05. The aim of changing this parameter was to change the velocity (because is inversely proportional with the Manning coefficient). The results are presenting at the next figure:


(a)

40 |
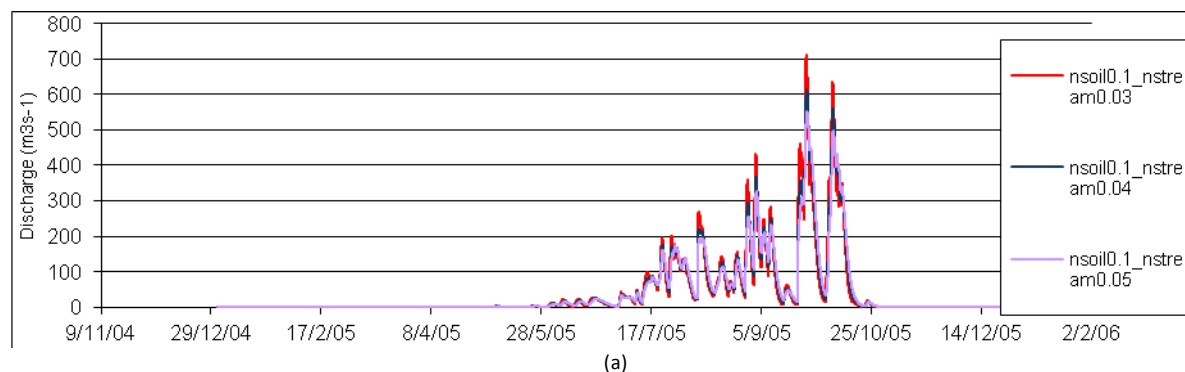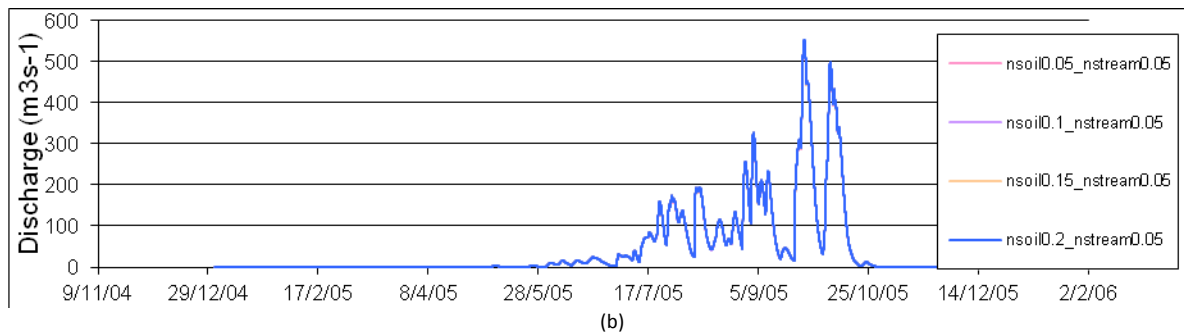
(b)

Fig. 29 Discharge with different Manning coefficients of soil and stream

With low values of the Manning coefficient, we have high peak at the discharge, while with high values lower peak. At this case the results present more smoothness. Moreover, another component that is affected also is the time of the peak as well. But this change doesn't affect the volume of the water volume. Something very important that carried out from the simulations is that changing the Manning coefficient of the soil, there is no influence at the streamflow (Fig.29). It is very strange in our case, because soil surface roughness is a critical parameter reflecting runoff processes and soil erosion, and is mainly influenced by soil surface characteristics. It is always used to describe the surface elevation variation, is a major factor influencing wind and water erosion, and can also be used to investigate runoff generation (Darboux F. et al., 2001).

Another parameter that has been selected to adjust was the vertical conductivity. It has been expected that by having lower values of this parameter has as consequence to produce exactly the same profile of discharge, but with higher peak but with change to the volume of the water. Lower values of the vertical conductivity provoke lower infiltration and Hortonian runoff, while higher values create more infiltration and then due to saturation from the lower layers, there is appearing exfiltration and no surface runoff. For the simulations, the reference values (that range between $4.87 \cdot 10^{-6}\ m/s$ and $5.5 \cdot 10^{-6}\ m/s$ for the three different soil classes) had been multiplied with the following factors: 0.01, 0.1, 1, 10 and 1000.
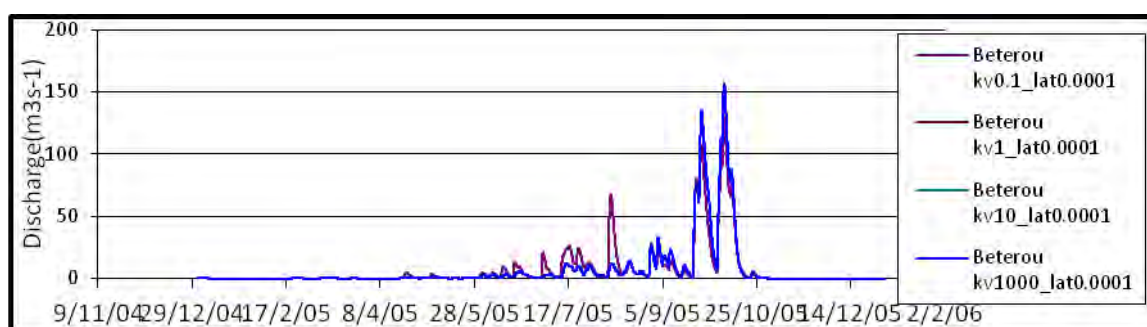
(a)
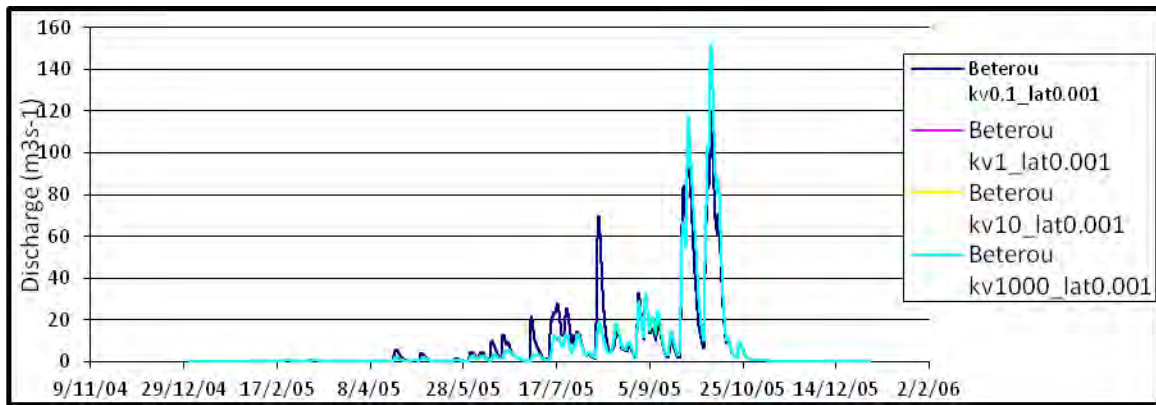
(b)
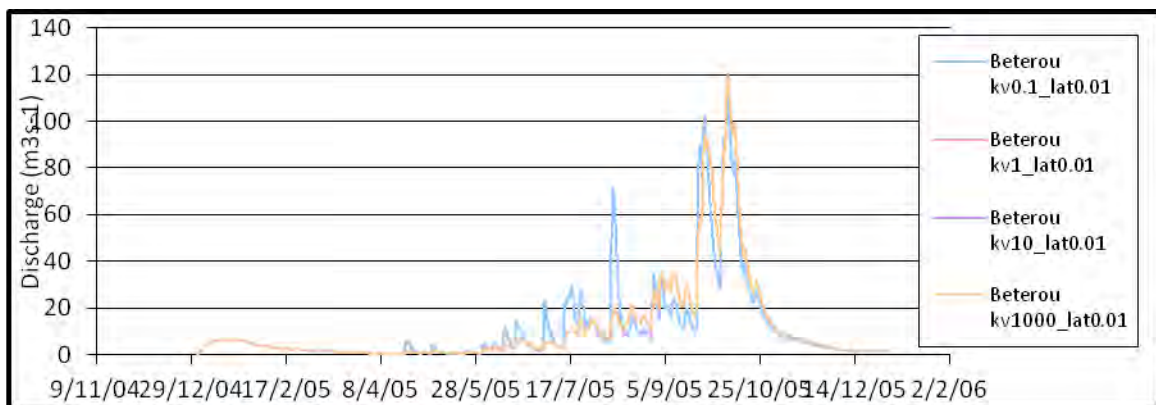
(c)

(d)

Fig. 30 Streamflow for different values of vertical conductivity (multiplied by different factor) for the year 2005
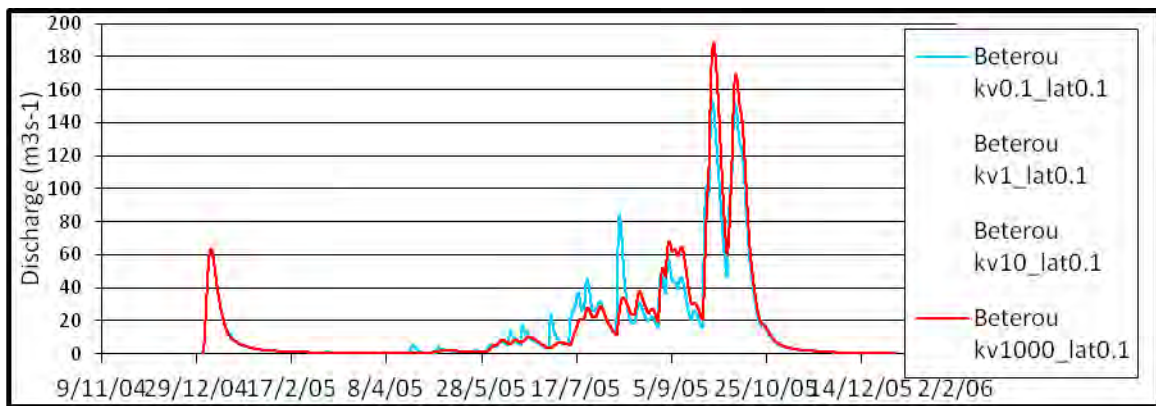
From the previous graphs (Fig. 30) and for the Beterou site, the simulations appear weakness to capture the same streamflow with the observation. It is more intense, for the time before September, where the observation data appear high discharge. Although the different values of the vertical conductivity that have been used, the streamflow at the beginning is low. Another thing that is strange, is the discharge that is appearing for vertical conductivity at the class of 10^{-3} m/s and lateral conductivity greater than 0.01. This streamflow at the beginning of the year, where there is no rainfall, may be caused because of saturation flow from a previous run. Contrary to Beterou site, the C238 is better represented by the model, although with an underestimation of the profile. For this site also, the better representative simulation, is with a class of 10^{-3} m/s.

Except of this parameter, another one that it was seemed to affect the streamflow, is the lateral conductivity. It influences subsurface flow rates, soil saturation and water table position, as well as the relative importance of subsurface runoff and saturation overland flow (Whitaker et al., 2003). At the DHSVM is assumed to be at a maximum at the land surface and taken to decline exponentially with the depth. If we have lower infiltration, then we have high lateral conductivity and then all the water goes to the river.
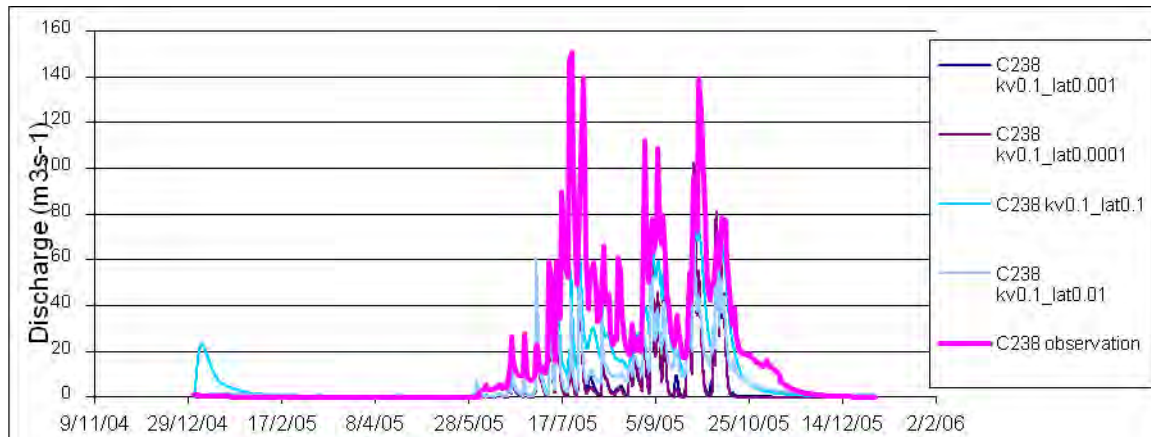

Fig. 31 Streamflow for different values of lateral conductivity for the year 2005

So, one way if we would like to increase the surface runoff is to increase the lateral conductivity. The values that were used for carrying out the simulations were: 0.0001, 0.001, 0.01, 0.1, 10 and 100. From the higher values (more than ten), there has been resulted that there is no influence and the simulations have been focused on the values of lower class.

5.3 Efficiency criteria

In this section, the efficiency criteria used in this study is presented and evaluated. The accuracy of the DHSVM model in simulating daily streamflow was evaluated using the coefficient of efficiency (Eff), the correlation coefficient (R^2), the root mean square error (RMS) and the BIAS.

The objective function that was used for the optimization was the Nash-Sutcliffe model efficiency (Nash & Sutcliffe, 1970):

$$Eff = 1 - \frac{\sum_{i=1}^{n}\left(Qobs_i - Qsim_i\right)^2}{\sum_{i=1}^{n}\left(Qobs_i - \overline{Qobs}\right)^2}$$

where, $Qobs_i$ is the observed flow on day i, $Qsim_i$ is the simulated flow on day i, $\overline{Qobs}$ is the average observed flow and n is the number of days for the simulation period. Nash-Sutcliffe efficiency can range from negative infinity up to 1. If there is E=1, it corresponds to a perfect match of modeled discharge to the observed data (and shows that the more accurate the model is). An efficiency of zero, indicates that the predictions of the model are as accurate as

the mean of the observed data, whereas value less than zero occurs when the observed mean is a better predictor than the model.

Efficiency criteria are defined as mathematical measures of how well a model simulation fits the available observations. In general, many efficiency criteria contain a summation of the error term (difference between the simulated and the observed variable at each time step) normalized by a measure of the variability in the observations.

As it was referred previously from the sensitivity analysis, there was not too much impact by changing the Manning's coefficient. So, hereafter are presenting the scores that derived by changing the values at the conductivities (vertical and lateral).

Vertical conductivity	Lateral conductivity	Accuracy Indicators			
		Correlation Coefficient	Efficiency Coefficient	RMS	BIAS
$\sim 10^{-7}$	0.0001	0.46	0.14	40.3	20.7
$\sim 10^{-6}$	0.0001	0.40	0.12	40.6	20.8
$\sim 10^{-5}$	0.0001	0.40	0.12	40.6	20.8
$\sim 10^{-3}$	0.0001	0.40	0.12	40.6	20.8
$\sim 10^{-7}$	0.001	0.49	0.15	40.0	20.4
$\sim 10^{-6}$	0.001	0.45	0.15	40.0	20.5
$\sim 10^{-5}$	0.001	0.45	0.15	40.0	20.5
$\sim 10^{-3}$	0.001	0.45	0.15	40.0	20.5
$\sim 10^{-7}$	0.01	0.60	0.27	37.0	17.4
$\sim 10^{-6}$	0.01	0.62	0.29	36.6	17.2
$\sim 10^{-5}$	0.01	0.62	0.29	36.6	17.2
$\sim 10^{-3}$	0.01	0.62	0.29	36.6	17.2
➡ $\sim 10^{-7}$	0.1	0.68	0.52	30.4	12.6
$\sim 10^{-6}$	0.1	0.62	0.52	30.6	11.9
$\sim 10^{-5}$	0.1	0.62	0.52	30.6	11.9
➡ $\sim 10^{-3}$	0.1	0.62	0.52	30.6	11.9
$\sim 10^{-7}$	1	0.65	-0.65	52.0	13.4
$\sim 10^{-6}$	1	0.58	0.51	30.6	6.7
$\sim 10^{-5}$	1	0.57	0.49	31.2	6.8
$\sim 10^{-3}$	1	0.57	0.49	31.2	6.8
$\sim 10^{-7}$	10	0.61	-18.47	170.1	66.5
➡ $\sim 10^{-6}$	10	0.53	0.15	38.1	4.8
$\sim 10^{-5}$	10	0.52	0.11	38.6	5.1
$\sim 10^{-3}$	10	0.52	0.11	38.6	5.1

Tab. 13 Scores of the accuracy indicators, by testing vertical and lateral conductivity

The values that appear at the previous table (Table 13) are the mean values of the two sites (for every indicator). Concerning the BIAS, we took the mean of the absolute values. From these scores, we can see that the best results appearing for lateral conductivity equal to 0.01, 0.1 and 1, with better score of vertical conductivity ranges at the classes of 10^{-7} m/s and 10^{-6} m/s (if we look at the values at the three first indicators, the correlation and the Nash-Sutcliffe efficiency have the higher scores and are denoted with the red arrows at the Table 13). The higher values that we have in correlation and Nash-Sutcliffe efficiency (with the best close to 1) denote good performance of our model. For the mean square error, the lower the values mean that we have best performance.

In contrary to this, if we look at the simulations by taking into account the BIAS, that indicate the model's overprediction (when BIAS<0) or underprediction (when BIAS>0) of streamflow (of course values equal to zero correspond to a perfect prediction), then the best simulation is with lateral conductivity equal to 10 and vertical conductivity at the classe of 10^{-6} as there are presented the smallest values of this indicator.
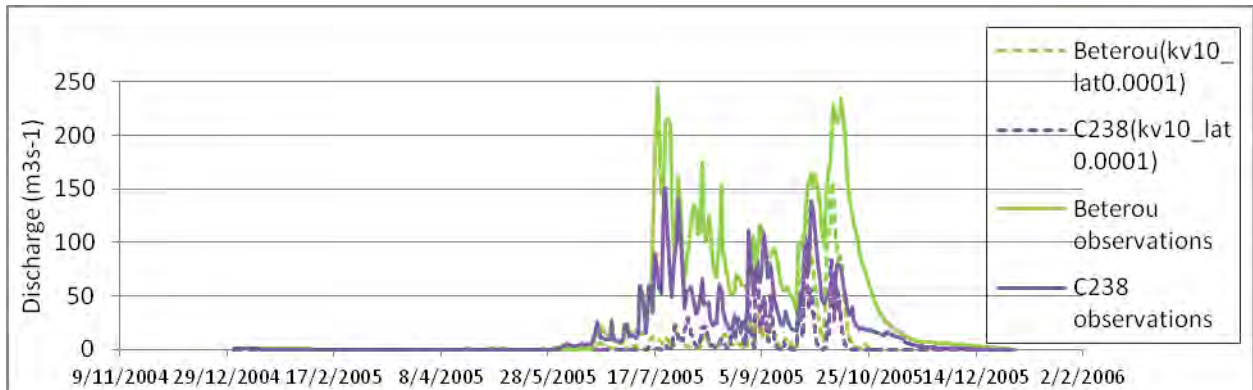
Fig. 32 Streamflow for vertical conductivity multiplied by the factor 10 and lateral conductivity equal to 0.0001 for the year 2005
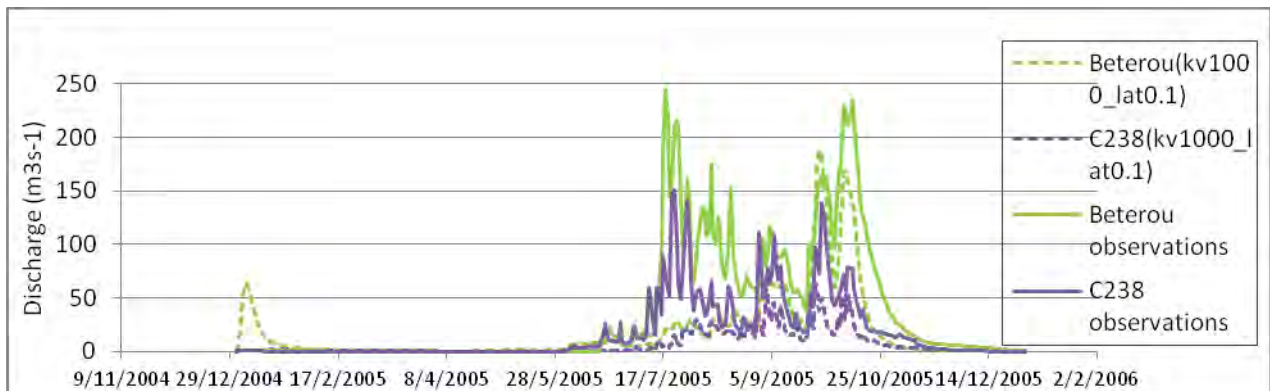
Fig. 33 Streamflow for vertical conductivity multiplied by the factor 1000 and lateral conductivity equal to 0.1 for the year 2005

At the previous figures (Fig. 32 and 33) is presented the streamflow for the two sites according to the best scores of the efficiency criteria.

For the vertical conductivity of class 10^{-5} and lateral conductivity 0.0001, the water table depth and the soil moisture are presented also.

Fig. 34 Water table depth for vertical conductivity ~10^{-5} and lateral conductivity equal to 0.0001 for the year 2005

45 |

Fig. 35 Soil moisture for vertical conductivity ~10^{-5} and lateral conductivity equal to 0.0001 for the year 2005

6. Conclusion and perspective

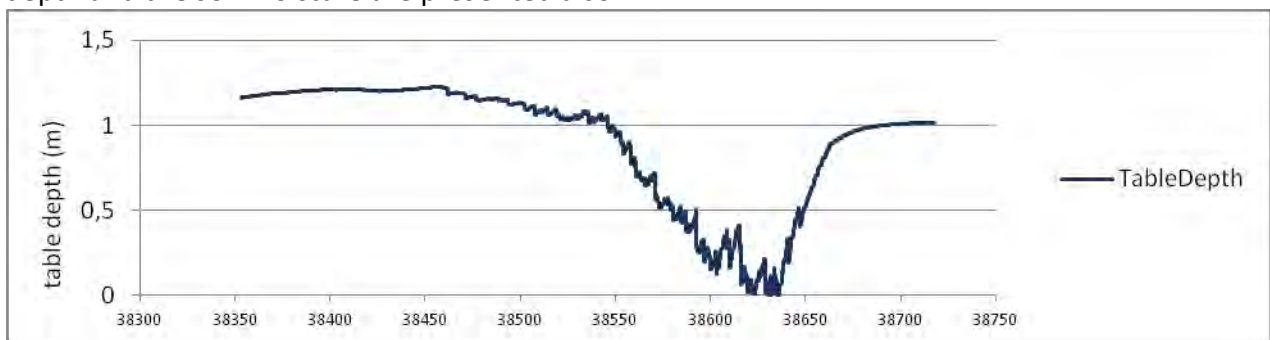At this study has been done an effort to test the ability of the hydrological DHSVM model to simulate hydrological processes in Benin catchment. The choice of this model at this area has been done for several reasons. This is a very good Land Surface Model, which has the advantage to take into account not only the vertical conductivity but also the lateral conductivity, so it has as consequence to be moved water from one pixel to another. Moreover, it is very good to simulate evapotranspiration and lateral fluxes, and of course is compatible for the processes that take place in Benin catchment. It uses a two layer representation of vegetation, something that it is very important in our case because the examination region is characterized by sparse vegetation and savanna. Last but not least, an additional supremacy of the selected model is that it simulates continuously the hydrological processes, either for example the existence of rain/snow or not.

It was the first time that this model applied at this region, so has been spend too much time and have been faced many difficulties that had to do with the knowledge of the necessary inputs for running the model. The nature of these problems had to do with the complexity of various parameters that concern the soil and the vegetation in this area, as well as with some technical difficulties inherent with the compatibility of the selected type of format. Another cause that provoked additional problems, was that it was used for the first time for this model the spatially distributed option for the forcing data (precipitation, temperature, e.t.c.). All the other times it was assumed that everything was homogeneous.

Some of these parameters derived either directly by computations from the available data (like the leaf area index and the albedo) or by the help of other functions (pedotransfer functions, with the use of a specific software). But there has been a great rate, especially for vegetation, that had been taken from bibliography. It is very important to find the accurate values of these parameters for taking good simulations because some of them affect a lot the results.

In our case study, the soil and vegetation classification has been separated in three classes. Another reasonable question, regarding the soil and vegetation separation at the selected classes could be set. Although the small differences of every class at the content of sand, clay and loam, as well as the fact that there has not been the same magnitude of pixels

46 |

according to the classification (at the third category there have been few, something that is not realistic in some values of the parameters that derive from the data), that maybe affect the results could not be different due to specific requirements of the ALMIP2 project.

For this reason, after having the first results there was the need to calibrate the model and change some parameters. The calibration and evaluation of the model has been performed for the year 2005, using streamflow records in two stations, where have been available data. Hydrologic studies show that stream discharge responses to climatic events are basin specific and are influenced by a number of factors (topography, soil distribution, bedrock type, forest cover) (Storck et al., 1995). Thus, a primary sensitivity analysis has been performed, to determine the model's ability to capture hydrologic processes within the watershed by changing some soil parameters and some parameters that had to do with the stream.

The initial results that derived from the first simulations in comparison with the validation data (concerning the streamflow) showed that there has been underestimation, especially in Beterou station. Due to lack of time, we achieved to test only four parameters which are more sensitive to streamflow. The idea was to play with the Manning coefficient (both of the stream and the soil) in order to change the peak of the discharge, without changing the volume of the water, as well as with the vertical and lateral conductivity (by affecting again the peak of the discharge by changing also the volume of the water)

The analysis in our case study showed that the Manning coefficient doesn't affect the results, while the changes in conductivity give better results, but appear again weakness to capture the same profile of the streamflow at the beginning of the year. In contrast, at the smallest site (C238), the performance of the model is better represented by the model. From the efficiency criteria it was found that we have better performance of the accuracy indicators for the lower values of lateral conductivity, and the best results with better correlation and efficiency are with vertical conductivity multiplied with a factor of 1 and 0.1. These slow values (of range between 10^{-7} m/s and 10^{-6} m/s) come in accordance with all the previous studies. The hydraulic conductivity determines the ability of the soil fluid, to flow through the soil matrix system under a specified hydraulic gradient. In our case study, there is sparse vegetation, so low values of the vertical conductivity have as consequence less infiltration and finally guide to more Hortonian runoff.

The sensitivity analysis provided insight into parameter influences. Another problem that has been resulted from the simulations is the mass balance error value. Not all precipitation reaching the land surface is available for streamflow or replenishing groundwater. Rather, a portion is temporarily stored by vegetation, where it is subject to evaporation. The total error has been computed from the model and is a measure to see how well the model was performing with the changes in some soil parameters. This mass balance error, which is the sum of the change in storage and the output (runoff and evapotranspiration) minus the input (precipitation), in our case and for the several simulations, had high values (up to 195mm).
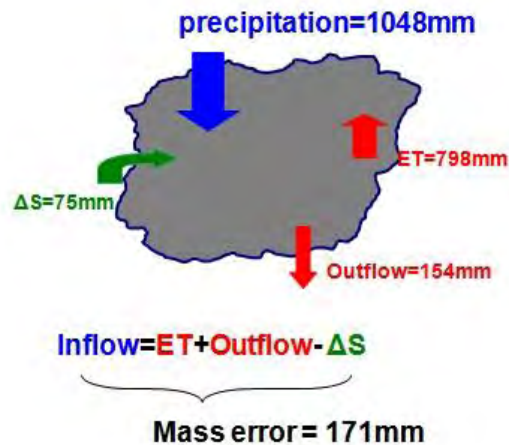
Fig. 36 Schematic representation of the mass balance error

An example with the schematic representation of the mass error, which is about 16% and corresponds to 171mm is given (Fig. 36).This fact reveals that model calculations were not performing adequately and maybe the water balance is not well simulated. Also, these high values maybe caused due to interfaces between the several equations that describe the physical processes (i.e. for the unsaturated moisture movement has been used Darcy's law, for the saturated subsurface flow a quasi 3D routing scheme (depends on water table depth, soil characteristics and topography), for evapotranspiration the Penman-Monteith formulation, e.t.c.).

Future efforts should focus on the components and the causes that are responsible for having high values of mass error. From the simulations, it was found that for high values of lateral conductivity (more than 1), there is observed very big reduction of the mass error, at about 100mm. An extensive sensitivity analysis is also required, not only for soil parameters but also for the vegetation parameters. Another important gap that has to be explained and corrected in the future is the problem with the fluxes and the net radiation that is appearing zero.

BIBLIOGRAPHIE

Bal H., Jannot Y., Quenette N., Chenu A., Gaye S.,(2012), "Water content dependence of the porosity, density and thermal capacity of laterite based bricks with millet waste additive", Construction and building materials, Volume 31, June 2012, p. 144-150

Boone A., Peugeot C., Demarty J., Grippa M., Benarrosh N., Brender P., Cappelaere B., Chaffard V., Charvet G., Chazarin J-P., Cloché S., Cohard J-M., Ducharne A., Fleury L., Galle S., Getirana A., Gosset M., Guichard F., Hiernaux P., KAptué A., Kergoat L., Lebel T., Maignan F., Mougin E., Ottlé C., Polcher J., Quantin G., Ramage K., Robert D., Roujean J-L., Séguis L., Timouk F., Velluet C., Viarre J., Vischel T., (2012), "AMMA Land Surface Intercomparison Project Phase 2: Meso to Local Scale", 4th International AMMA Conference, June 2-6, 2012, Toulouse

Bristow K.L., (1998), "Measurement of thermal properties and water content of unsaturated sandy soil using dual-probe heat-pulse probes", Agricultural and forest meteorology, 89 (1998), p. 75-84

Cuo L., Giambelluca W., Ziegler A., Nullet M., (2008), "The roles of roads and agricultural land use in altering hydrological processes in Nam Mae Rim watershed, northern Thailand", Hydrological processes, Volume 22, p.4339-4354

Cuo L., Lettenmaier D., Mattheussen B., Storck P., Wiley M., (2008), "Hydrologic prediction for urban watersheds with the Distributed Hydrology soil Vegetation Model", Hydrological processes, Volume 22, p.4205-4213

Darboux F., Davy Ph., Gascuel-Odoux C., Huang C., (2001), "Evolution of soil surface roughness and flowpath connectivity in overland flow experiments", Catena, Volume 46, p.125-139

Doten C., Bowling L., Lanini J., Maurer E., Lettenmaier D., (2006) , "A spatially distributed model for the dynamic prediction of sediment erosion and transport in mountainous forested watersheds", Water resources research, Volume 42, W04417

Doten C., Lettenmaier D., (2004), "Prediction of sediment erosion and transport with the Distributed Hydrology Soil Vegetation Model ", Water resources series, Technical report, No 178

Giertz S., Diekkrüger B., (2003), "Analysis of the hydrological processes in a small headwater catchment in Benin (West Africa)", Physics and Chemistry of the Earth, Volume 28, p.1333-1341

Giertz S., Diekkrüger B., Steup G., (2006) "Physically based modelling of hydrological processes in a tropical headwater catchment (West Africa)-process representation and multi-criteria validation", Hydrology and earth system sciences, Volume 10, p.829-847

Hall R., (2002), "Aerodynamic resistance of coppiced poplar", Agricultural and Forest Meteorology, Volume 114, Issues 1-2, December 2002, p. 83-102

Jie Song, (1998), "Diurnal asymmetry in surface albedo", Agricultural and forest meteorology, Volume 92, Issue 3, October 1998, p.181-189

Josef Kellndorfer, Wayne Walker, Leland Pierce, Craig Dobson, Jo Ann Fites, Carolyn Hunsaker, John Vona, Michael Clutter, (2004), "Vegetation height estimation from Shuttle Radar Topography Mission and National Elevation Datasets", Remote sensing of environment, Volume 93, Issue 3, November 2004, p. 339-358

Lhomme J., Elguero E., Chehbouni A., Boulet G., 1998, "Stomatal control of transpiration : Examination of Monteith's formulation of canopy resistance", Water resources research, Volume 34, No 9, p.2301-2308

Lipiec J., Usowicz B., Ferrero A., (2007), "Impact of soil compaction and wetness on thermal properties of sloping vineyard soil", International Journal of heat and mass transfer", Volume 50, Issues 19-20, September 2007, p. 3837-3847

Peugeot C., Guichard F., Bock O., Bouniol D., Chong M., Boone A., Cappelaere B., Gosset M., Besson L., Lemaitre Y., Séguis L., Zannou A., Galle S., Redelsperger J., (2011), "Mesoscale water cycle within the West African Monsoon", Atmospheric science letters, 12, p.45-50

Safeeq M., Fares A., (2011), "Hydrologic response of a Hawaiian watershed to future climate change scenarios", Hydrological processes

Séguis L., Boulain N., Cappelaere B., Cohard J., Favreau G., Galle S., Guyot A., Hiernaux P., Mougin E., Peugeot C., Ramier D., Seghieri J., Timouk F., Demarty J., Descroix L., Descloitres M., Grippa M., Guichard F., Kamagaté B., Kergoat L., Lebel T, Le Dantec V., Le Lay M, Massuel S., Trichon V., (2011), "Contrasted land-surface processes along the West African rainfall gradient", Atmospheric science letters, 12, p.31-37

Séguis L., Kamagaté B., Favreau G., Descloitres M., Seidel J., Galle S., Peugeot C., Gosset M.,Le Barbé L., Malinur F., Van Exter S., Arjounin M., Boubkraoui S., Wubda M., (2011), "Origins of streamflow in a crystalline basement catchment in a sub-humid Sudanian zone: The Donga basin (Benin, West Africa) Inter-annual variability of water budget", Journal of hydrology, 402, p. 1-13

Storck P., Bowling L., Wetherbee P., Lettenmaier D., (1998) , "Application of a Gis-base distributed hydrology model for prediction of forest harvest effects on peak stream flow in the Pacific Northwest", Hydrological processes, Volume 12, p.889-904

Tao He, Shunlin Liang, Dongdong Wang, Hongyi Wu, Yunyue Yu, Jindi Wang, (2012), "Estimation of surface albedo and directional reflectance from moderate resolution imaging spectroradiometer (MODIS) observations", Remote sensing of environment, Volume 119, April 2012, p.286-300

Thanapakpawin P., Richey J., Thomas D., Rodda S., Campbell B., Logsdon M., (2006), "Effects of landuse change on the hydrologic regime of the Mae Chaem river basin, NW Thailand", Journal of hydrology, Volume 334, p.215-230

VanShaar J., Haddeland I., Lettenmaier D., (2002), "Effects of land cover changes on the hydrological response of interior Columbia River basin forested catchments", Hydrological processes, Volume 16, p.2499-2520

Waichler S., Wemple B., Wigmosta M., (2005), "Simulation of water balance and forest treatment effects at the H.J.Andrews Experimental Forest ", Hydrological processes, Volume 19, p.3177-3199

Waichler S., Wigmosta M.,(2003) , "Development of hourly meteorological values from daily data and significance to hydrological modelling at H. J. Andrews Experimental Forest", Journal of hydrometeorology, p.251-263

Whitaker A., Alila Y., Beckers J., Toews D., (2003), "Application of the Distributed Hydrology Soil Vegetation Model to Redfish Creek, British Columbia: model evaluation using internal catchment data", Hydrological processes, Volume 17, p.199-224

Wigmosta M., Vail L., Lettenmaier D., (1994), "A distributed hydrology-vegetation model for complex terrain", Water resources research, Volume 30, No 6, June 1994, p.1665-1679

Wigmosta M.S., Nijssen B., Storck P. (2002), "Mathematical models of small watershed hydrology and applications: the Distributed Hydrology Soil Vegetation model", Water Resource Publications, Littleton, p.7-42

Yuan F., Bauer M., (2007), "Comparison of impervious surface area and normalized difference vegetation index as indicators of surface urban heat island effects in Landsat imagery", Remote Sensing of environment, Volume 106, Issue 3, February 2007, p. 375-386

OSUG

Université
Joseph Fourier
GRENOBLE
UFR PhITEM

Master Sciences de la Terre et de l'Environnement

Non-plagiarism certificate

I, the undersigned [First name, FAMILY NAME]

Eleni KOLOKYTHA
....

Author of the report entitled [Title]

Implementation of the Distributed Hydrological Soil Vegetation Model (DHSVM) in West Africa: ALMIP Phase 2 project
....

....

....

Declare that the above-cited report results from my personal work and that I have neither forged, falsified nor copied all or part of another persons work to present it as mine.

All sources of information used and all author citations have been included following standard usage.

I am aware of the fact that failing to cite a source or failing to cite it fully and properly constitutes plagiarism, and that plagiarism is considered a serious offence within the university that can be sanctioned severely by law.

At (place) Grenoble
....

the (date) 07/01/2013
....

Student's signature